DANMARKS OG GRØNLANDS GEOLOGISKE UNDERSØGELSE RAPPORT 2019/24

The risk of scaling and corrosion predicted formation water composition for Danish geothermal plants

Jolanta Kazmierczak, Nicolas Marty,
Hanne D. Holmslykke & Rikke Weibel

GEOLOGICAL SURVEY OF DENMARK AND GREENLAND
DANISH MINISTRY OF CLIMATE, ENERGY AND UTILITIES

GEUS

DANMARKS OG GRØNLANDS GEOLOGISKE UNDERSØGELSE RAPPORT 2019/24

The risk of scaling and corrosion predicted formation water composition for Danish geothermal plants

Jolanta Kazmierczak, Nicolas Marty,
Hanne D. Holmslykke & Rikke Weibel

GEOLOGICAL SURVEY OF DENMARK AND GREENLAND
DANISH MINISTRY OF CLIMATE, ENERGY AND UTILITIES

Dansk sammenfatning

Udfældning af mineraler eller korrosion kan skabe vanskeligheder for produktionen af geotermisk energi. Den kemiske sammensætning af det varme vand i undergrunden har stor betydning for hvilke mineraler, der eventuelt kan udfældes i et geotermisk anlæg. Derfor er geotermisk vand blevet udtaget fra produktions- og injektionsboringer ved de tre danske geotermiske værker: Margretheholm, Sønderborg og Thisted. Vandets sammensætning af hoved- og sporelementer er analyseret. Geokemisk modellering ved brug af programmerne MARTHE-PHREEQC og PHREEQC er anvendt til at vurdere, hvilke mineraludfældninger, der udgør den største risiko. Sammensætningen af sandstensreservoirerne er sammenlignet med vandkemien for at vurdere, hvilke mineralogiske ændringer der kan forventes, når afkølet vand returneres til reservoiret. Den geokemiske modellering har vist at risiko for udfældninger i reservoiret i Thisted og Sønderborg er begrænset. Der kan forventes udfældning af baryt efter afkøling af formationsvandet ved Margretheholm, hvilket kan reducere injektiviteten. Øvrige udfældninger samt en forventet omdannelse af nogle mineraler til ler forventes at have ubetydelig påvirkning af reservoiret.

Extended summary

Precipitation of solids, i.e. scaling, from geothermal water is a commonly experienced problem. Formation water may contain soluble species in concentrations up to 300 g/L. During production of geothermal water, the change in temperature and pressure may lead to precipitation of solids (scaling) and/or corrosion in the plant facilities. Scaling and corrosion may jeopardise geothermal energy production by reducing the injectivity from the injection well to the reservoir or destruction of the well casing, pipes and plant equipment. This study addresses the risk of scaling in Danish geothermal plants (Margretheholm, Sønderborg and Thisted) based on geochemical modelling of formation water from these plants. The present report is one of the final reports of WP3 under the project GEOTHERM – Geothermal energy from sedimentary reservoirs – Removing obstacles for large scale utilization supported by the Innovation Fund Denmark: project 6154-00011B.

Formation water was sampled during operation of the Margretheholm, Sønderborg and Thisted geothermal plants from both the production well and close to the injection well, and the chemical composition of the brine was measured. The potential risk of scaling was modelled by MARTHE-PHREEQC, which considers the potential for mineral precipitation in the reservoir in a radial flow from the injection well. The Pitzer database was applied in order to address the very saline formation water; however, the drawback with this database is that silicate precipitation cannot be considered. Therefore, additional reactive transport modelling was performed using PHREEQC and its phreeqc database to include a larger range of minerals in the evaluation of potential geochemical reactions upon injection of cooled formation water. Input parameters were besides mineralogy and porosity of the reservoir, formation water composition and production data such as depth of well head, formation water temperature, flow rates etc. Furthermore, the risk of barite nucleation in the injection wells was modelled. The modelling only addresses the risk of scaling and thus several processes such as the formation of biofilm, corrosion processes and transport of particles have not been taken into account because of lack of data in the model databases and current software capabilities (e.g. transport of eroded particles).

The results of the modelling show that very small amounts of minerals are expected to precipitate at Sønderborg and Thisted geothermal plants and that the precipitates most likely do not affect the injectivity of the reservoir. In contrast, the production and injection water compositions from the Margretheholm plant suggest barite and celestine precipitation after the heat extraction. Precipitation of celestine is modelled to occur c. 50-100 m from the injection well and is therefore not expected to affect the reservoir properties. Precipitation of barite on the other hand occurs instantaneously whether the process is modelled in the injection well or in the reservoir. It is thus unclear whether barite precipitates immediately after cooling of the formation water in the heat exchanger. If the barite particles are not captured in the filters in the geothermal plant before injection into the reservoir, such particles may affect the injection of cooled water by clogging the porosity of the reservoir rock.

Results of the reactive transport model calculations conducted in PHREEQC indicate additional reactions likely to take place in the reservoir sandstones close to the injection of cooled water. The mineral reactions include transformation of dolomite to calcite and alteration of K-feldspar into chlorite and/or kaolinite. These processes, however, should have minor influence on the reservoir permeability.

The likeliness of corrosion is indicated by increased iron and/or zinc content in the formation water after cooling. This is evident from the Sønderborg and Margretheholm geothermal plants. At Margretheholm, the increase of iron content in the cooled formation water is accompanied by a reduction in the lead content due to precipitation of metallic lead. Unfortunately, electrochemical reactions were not possible to evaluate with the applied geochemical modelling programs.

Future investigations of formation water ought to continue the initiated detailed analyses of major and trace elements. A detailed study of the potential for barite nucleation in the reservoir, including laboratory core flooding experiments, could provide essential information for the evaluation of the risk of barite precipitation at the injection wells and its potential detrimental effect on the injectivity. Measurements of stable isotopes and radiogenic isotopes could provide valuable information for better understanding the evolution from depositional to formation water and the possible mixing between formation water of different composition. This would allow an improved prediction of formation water composition in undrilled areas and help to take actions against potential scaling risks.

Content

1. Introduction

The presented results from geochemical modelling of formation water addresses the risk of scaling and corrosion for Danish geothermal plants. The report thereby finalizes the reporting of Milestone 3.6c in WP 3 of the project GEOTHERM – Geothermal energy from sedimentary reservoirs – Removing obstacles for large scale utilization supported by the Innovation Fund Denmark: project 6154-00011B.

The purpose of this study is to address the risk of scaling and corrosion at Danish geothermal plants by geochemical modelling. The reservoir sandstone and formation water composition are different for the three Danish geothermal plants, Thisted, Sønderborg and Margretheholm, hence variation in potential risks of scaling and corrosion can be expected. A major part of this concerns the effect of water cooling and the resulting mineralogical transformations/precipitations, which has been investigated through cooperation between GEUS and BRGM (the French Geological Survey). The findings from the Danish geothermal plants are compared with production and injection problems experienced at geothermal plants in France, Germany and Sweden (Table 1.1, 1.2, 1.3; Erlström 2017; Pastrik and Förster 2017; Tremosa et al. 2017). The comparison focuses on low (< 100°C) to medium (~150°C) enthalpy geothermal plants exploiting siliciclastic reservoirs.

Formation water contain various quantities of soluble species (up to 300 g/mL) and dissolved gasses (e.g. Andritsos et al. 2002; Bozau et al. 2015; Holmslykke et al. 2019). The changed thermodynamic conditions (in particular lowered temperature and pressure) during production reduce the solubility of most minerals and increase the risk of precipitation (i.e. scaling), corrosion of metal surfaces in contact with the fluids, and occasionally even emission of harmful gasses (e.g. Andritsos and Karabelas 1991; Andritsos et al. 2002; Nitschke et al. 2014; Wanner et al. 2017; Demir et al. 2019). In addition, precipitating minerals may incorporate naturally occurring radioactive nuclides and therefore may be a potential hazard to health and environment (e.g. Nitschke et al. 2014). Microbial induced precipitations are yet another type of scaling (e.g. Nitschke et al. 2014).

Scaling may occur anywhere in the geothermal system, in the geothermal wells, the reservoir rock, surface facilities, reinjection line etc. The composition of scaling depends on several parameters, such as temperature, pressure, formation water composition, reservoir rock and the operating conditions. Calcium carbonate is one of the most common scaling types in low – medium (< 150°C) enthalpy geothermal waters, whereas silica scale precipitates from high temperature, low salinity fluids (e.g. Andritsos et al. 2002; Wanner et al. 2017; Demir et al. 2019). In particular, carbonate scaling forms due to CO_2 degasification.

Heavy metals sulphides precipitate due to a combination of factors, such as pH increase as CO_2 degases, and temperature drop, since the solubility of sulphides increases with temperature (Andritsos & Karabelas 1991; Nitschke et al. 2014). Corrosion of steel is an important source of iron that may facilitate iron sulphide precipitation. Sulphide is formed by bacterial reduction of sulphate in the formation water.

In France, 13 low – medium enthalpy geothermal plants applying siliclastic reservoir rocks frequently encountered problems with the reinjection of geothermal water, and only those using sandstone reservoirs at shallow depths (600 to 1200 m) were successful (Trémosa et al. 2017).

Table 1.1: Production and injection problems experienced at the Lund geothermal plant in Sweden (Erlström 2017).

Plant	Reservoir sandstone	Fluid composition (mg/l)		Injection problems
Lund, Sweden	Upper Cretaceous, Lund Sandstone Fm Quartz (85%), feldspar (1-5%), glauconite (rare), carbonate grains (rare) Carbonate cemented	**Cl**	38000 35800	Corrosion of the casing due to incorrect ESP installation Minor scaling of unknown composition
		SO_4	20 1.0	
		COD	1220 2030	
		NH_4	27.8 20.5	
		NO_2	<0.002 <0.002	
		Ni	<0.005 <0.008	
		Fe	38.4 53.0	
		K	87 88	
		Si	6.2 6.1	
		Al	0.40 0.32	
		Sr	1350 1050	
		Ca	7200 6500	
		Na	13100 13400	
		Cu	0.07 0.10	
		Mn	0.23 0.24	
		Pb	1.00 0.04	
		Ag	0.11 0.09	
		Mg	1130 980	

Table 1.2: Production and injection problems experienced at different geothermal plants in France (compiled from Tremosa et al. 2017).

Plant	Reservoir sandstone	Fluid composition (mg/l)		Injection Problems
Melleray, France	Rhaetian? Calcite (abundant), dolomite (frequent), quartz (frequent), smectite (frequent), illite or muscovite (frequent), kaolinite (rare), feldspar (rare)	**Ca**	1166	Clay clogging (Sulphate-reducing bacteria) (Saturation index suggests equilibrium with calcite and dolomite)
		Mg	374	
		Na	10900	
		K	309	
		HCO_3	305	
		Cl	19738	
		SO_4	1800	
		NH_4	13	
		SiO_2	37	
		Ba	<1	
		Li	13.1	
		Rb	0.3	
		Sr	41.2	
		Mn	0.42	
Achéres and Cergy-Pontoise, France	Triassic / Dogger formations			Injection problems with Triassic sandstones unsolved. Geothermal reservoir changed to oolithic Dogger Formation.
Bordeaux, France	Turonian, Cenomanian sand and limestone			No reinjection!

Châteauroux, France	Triassic sandstone	**Na** **Ca** **HCO_3** **SO_4** **Fe**	47.7 18.2 201 14.6 0.06	No injection well.

Table 1.3: Production and injection problems experienced at different geothermal plants in Germany (compiled from Pastrik and Förster 2017).

Plant	Reservoir sandstone	Fluid composition (mg/l)		Injection problems
Neustadt-Glewe, Germany	Rhaetian Contorta Sandstone Quartz (94%), feldspar (3%), calcite (0.5%), dolomite + siderite (1 %) Cement includes pyrite, anhydrite, halite, quartz, dolomite, kaolinite	**K** **Na** **Ca** **Mg** **Fe** **Mn** **NH4** **Ba** **Cu** **Li** **Sr** **Cl** **Br** **I** **SO4** **HCO3**	782 80010 8409 1410 60.0 10.0 - - 0.053 8.3 440 137000 390 - 470 40	Corrosion, mainly electrochemically driven. Bacteria play a minor role. Scaling due to degassing. Solid precipitate consists of iron-hydroxides, galenite, celestine-barite (radioactive).
Neubrandenburg, Germany	Upper Triassic Exter Fm and Contorta Sandstone Quartz (89%), feldspar (4%), kaolinite (3%), calcite (1%), dolomite (0.5%), pyrite (rare), chlorite (rare). Carbonate, quartz and kaolinite cement.	**K** **Na** **Ca** **Mg** **Fe** **Mn** **NH4** **Ba** **Cu** **Li** **Sr** **Cl** **Br** **I** **SO4** **HCO3**	186 48000 2000 631 12.6 0.73 28.8 0.46 0.024 - 107 82000 182 11 1020 159	Corrosion and precipitation (lead and copper compounds) due to microorganisms and bimetallic elements. Corrosion and scaling was significantly increased after stagnant phases.
Waren / Müritz, Germany	Rhaetian Exter Fm (production well) / Hettangian (injection well) Quartz (90%), feldspar (6%), kaolinite/illie (2%), calcite (0.5%), dolomite-siderite (0.5%) Dolomite and quartz cement	**K** **Na** **Ca** **Mg** **Fe** **Mn** **NH4** **Ba** **Cu** **Li** **Sr** **Cl** **Br** **I** **SO4** **HCO3** **NO3** **HPO4**	264 57650 2730 780 15.8 1.46 30 0.61 0.003 - 148 95615 177 6 900 163 1.2 0.06	Avoided by filtering and adding nitrogen to the system.

Neurup-pin, Ger-many	Lower Dogger Aalen Sand-stone	**K** 446 **Na** 74700 **Ca** 1540 **Mg** 1070 **Fe** 31 **Sr** 44 **Mn** 1.2	Injection-problems due to flow behind the casing!
Hannover, Germany	Triassic Bunter Sandstone Fm Quartz-dominated, mica-ceous, carbonatic sand-stones.	**Ba** 59 **BO2** 302 **Br** 945 **Ca** 29582 **Cl** 171825 **Fe** 92 **HCO3** 121 **K** 4581 **Li** 124 **Mg** 1384 **Mn** 190 **Na** 69084 **Pb** 81 **SiO2** 73 **SO4** 1026 **Sr** 1554	Halite precipitation.

2. Danish geothermal plants

2.1 Margretheholm

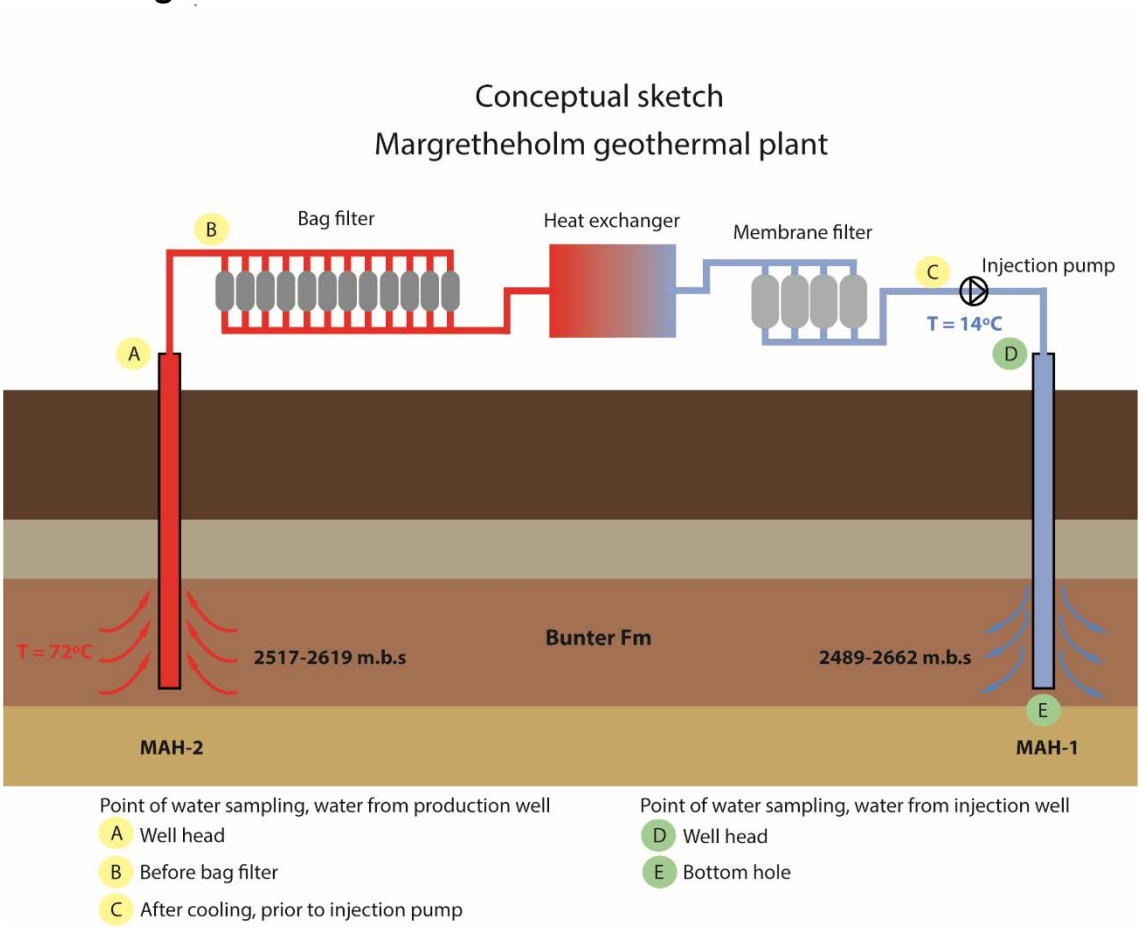

Figure 2.1: *Conceptual sketch of the water flow in Margretheholm geothermal plant on Amager from production well (MAH-2) through the bag filter (posefiltre), heat exchanger, membrane filter (patronfiltre), and to the injection well (MAH-1). Modified from https://www.geothermperform.eu.*

Hovedstadens Geotermiske Samarbejde (HGS), a consortium of VEKS, CTR, HOFOR and DONG initiated the two wells (MAH-1 and MAH-2) in 2003 and 2004. The Margretheholm geothermal plant started operation in 2005 (Figure 2.1; Dansk Fjernvarme 2019).

The three absorption heat pumps were driven by steam from the Copenhagen Steam Distribution System, which in 2008 was changed to water-based district heating, or alternatively by the Amagerværk (Dansk Fjernvarme 2019). 230 m^3/hour can be produced from the production well with a wellhead at 2600 m's depth (Dansk Fjernvarme 2019). In reality, the typical production was 130 m^3/hour with a maximum of 200 m^3/hour (Carsten Møller pers.

comm., 2019). The water temperature in the reservoir is 72°C. After cooling in the heat exchangers, the water is injected with a temperature of 17°C (Dansk Fjernvarme 2019). The geothermal plant produces annually up to 300.000 GJ equal to the consumption of 4600 households (Dansk Fjernvarme 2019).

Reservoir rock

The reservoir is in the Lower Triassic Bunter Sandstone Formation, which was deposited in an arid climate mainly from braided streams and aeolian activity (Clemmensen 1985, Olsen 1987).

The mineralogical composition of the Bunter Sandstone Formation from the Margretheholm area has been evaluated from cuttings samples by Mineralscan and hence is not equally well defined as for e.g. the Thisted area. The Bunter Sandstone Formation consists here mainly of quartz (57 vol%), abundant K-feldspar (25 vol%) and common plagioclase (5 vol%) (Olivarius et al. 2018). Rock fragments are not identified by the Mineralscan method but are typically common in the Bunter Sandstone Formation (Weibel and Friis 2004). Heavy minerals are rare (< 1 vol%), which is comparably low for the Bunter Sandstone Formation elsewhere in Denmark. The cementing phases are mainly calcite (4 vol%), dolomite (3 vol%) and rare clay minerals.

An average porosity of 22% has been interpreted from petrophysical logs, and corresponding permeabilities of 300 mD have been estimated from general porosity – permeability relationship (Vosgerau et al. 2015c; Kristensen et al. 2016).

Production problems

Acid treatment was considered as a solution to the occasional pressure build-up in the injection well. The effect of acid treatment on the reservoir was investigated (Laier and Weibel 2011). Laboratory tests showed a potential risk of releasing fine particles by this treatment.
Camera inspection of the well showed clogged perforations, and bailer sampling showed that the well was partly filled with metallic (lead) grains and siliciclastic sand (Laier 2014). Analysis of particles suspended in water collected at the membrane filters contained few silicate minerals and some iron oxides (Laier 2015a). The particle concentration was highest (50 mg/L) after pauses in the production and decreased to 0.5 mg/L during continued production. Lead particles were identified in bag filter, tubing and electrical submersible pumps, indicating galvanic reactions occurring in the plant facilities (Laier 2015b, 2015c, 2015d). Deposition of metallic lead by galvanic corrosion of steel reduces injectivity (Laier 2015d; Olivarius et al. 2018; Mathiesen 2019). Application of corrosion inhibitor has limited effect according to on-site and laboratory tests (Mathiesen 2019). Several sources for lead in well and plant facilities have been considered, e.g. both lead and radioactive lead are present in the Bunter Sandstone Formation, mainly in zircon grains (Olivarius et al. 2018).

2.2 Sønderborg

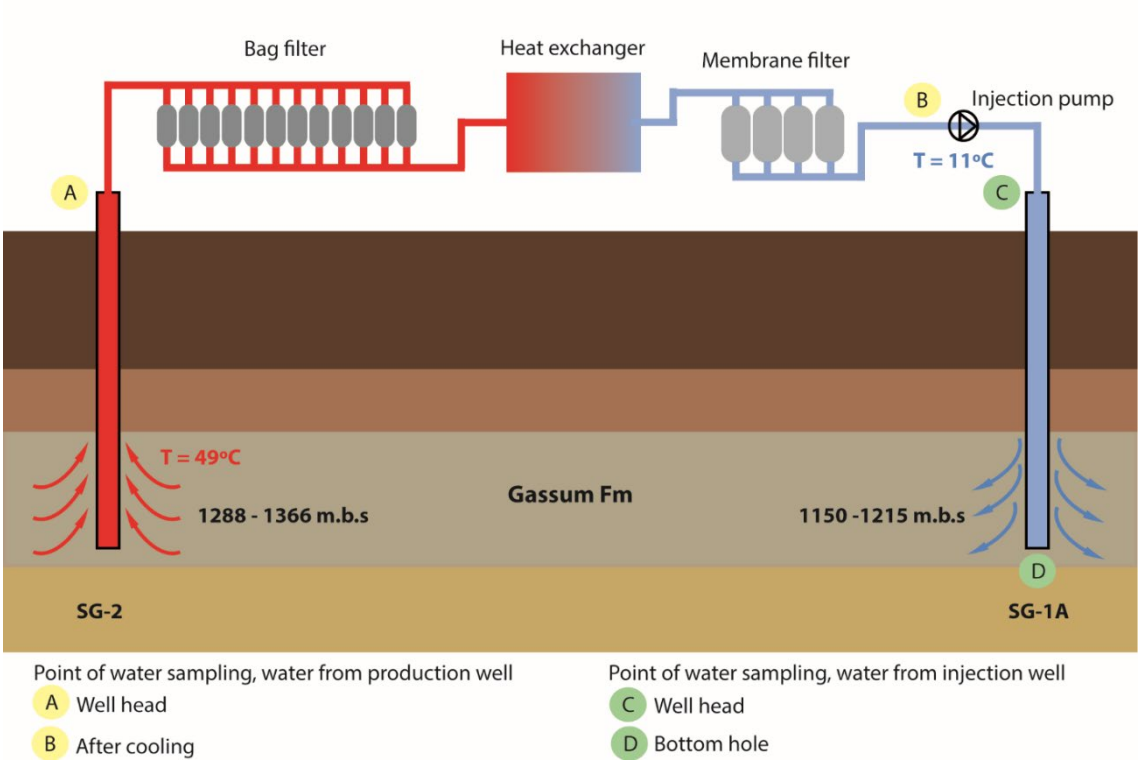

Figure 2.2: *Conceptual sketch of the water flow in Sønderborg geothermal plant from production well (SG-2) through the bag filter (posefiltre), heat exchanger, membrane filter (patronfiltre) and to the injection well (SG-1A). Modified from https://www.geothermperform.eu.*

The geothermal exploration wells, Sønderborg-1 and -2, were drilled in 2008 and 2010. Dansk Fjernvarmes Geotermiselskab assisted Sønderborg Fjernvarme with establishing the geothermal plant in 2013 (Figure 2.2).

Heat for the absorption heat exchangers is provided from combustion of wood chips. The plant has a capacity of 12.5 MJ/s equal to annually 394.000 GJ, which approximately corresponds to the annual heat demand from 2400 households (Dansk Fjernvarme 2019; Energistyrelsen 2019). The plant is planned to be in operation only during the winter.

The water temperature in the reservoir at 1300 m is 45°C and after cooling in the heat exchangers the injection water temperature is planned to reach c. 8°C, but is in reality 15–20°C (Vosgerau et al. 2015b; Mathiesen 2019).

Reservoir
The reservoir is in the Upper Triassic–Lower Jurassic Gassum Formation, which was deposited under a humid climate in paralic and marine depositional environments (Nielsen 2003).

The Gassum Formation at Sønderborg contains abundant quartz (56-57 vol%), common mica (22 vol%), minor amounts of K-feldspar (3-4 vol%) and plagioclase (1-2 vol%) and rare heavy minerals (< 1 vol%). Cementing phases comprise calcite (8-9 vol%), pyrite and anatase (< 1 vol%). Rare to abundant kaolinite (2-18 vol%) may comprise both clay clasts and cementing phases.

The reservoir has a porosity of 28 %, which is calculated from petrophysical logs and an estimated permeability of 2800 mD (Vosgerau et al. 2015b).

Production problems

The exact mechanisms for the injectivity problems at Sønderborg Geothermal plant is still unknown, but several causes have been proposed. Clogging of filters has been suggested to be caused by rust and impurities in the formation water (Energy Supply 2016).

Injection problems in June 2014 were documented by camera inspection to be caused by flakes in the filter probably corrosion flakes (Laier 2016). Clean-up operation of the well increased the injection rate only temporally. High corrosion rates of steel are observed at the injection well (Mathiesen 2019). This combined with mill scales on the inside of all tubing may result in severe release of rust flakes and plugging of the well (Mathiesen et al. 2019).

The water in the geothermal plant contained suspended material of zink-sulphide and lead-sulphide (Laier 2015). Zink and lead may have been sourced from material applied in the well (e.g. pipe dope) and at the plant (e.g. lead added to steel to improve machinability) whereas sulphide could have formed by bacterial reduction of sulphate (Laier 2015, 2016). DNA from sulphate reducing bacteria related to *Desulfotomaculum halophilum* are identified in bag filters from the plant (Laier 2016).

It has also been proposed that the injectivity problems at Sønderborg geothermal plant are caused by a non-optimal installation of the gravel packs which causes heavy impairment of the wells with well skins > 30 (van der Post 2019). This initial impairment is then made worse by the scaling and corrosion problems that the well has suffered throughout its injection life.

2.3 Thisted

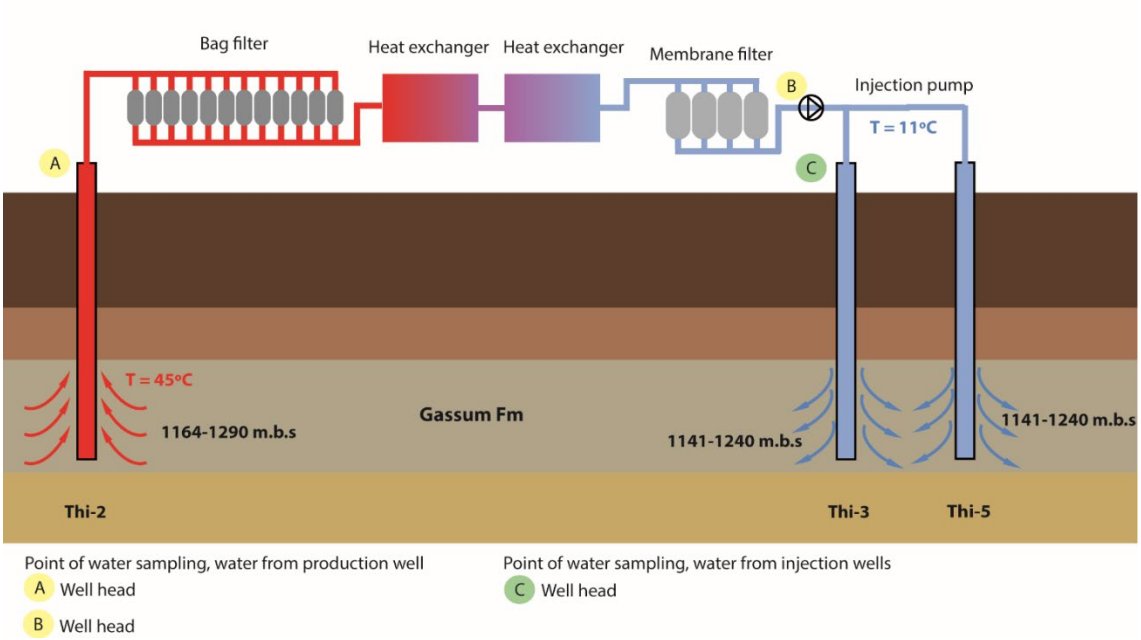

Figure 2.3: *Conceptual sketch of the water flow in Thisted geothermal plant from production well (Thi-2) through the bag filter (posefiltre), heat exchangers, membrane filter (patronfiltre) and to the injection wells (Thi-3, Thi-5). Modified from https://www.geothermperform.eu.*

History and capacity

The exploration wells Thisted-2 and -3 were drilled by DONG in 1982 and 1983, respectively (Nielsen and Japsen 1991). Thisted Varmeforsyning operates the geothermal plant, which has been in operation since 1984 as the first and oldest geothermal plant in Denmark (Figure 2.3; Dansk Fjernvarme 2019).

The originally electrically driven heat pump was in 1988 replaced by an absorption heat pump due to changed electricity regulations. In 2000, the plant was expanded by an additional absorption heat pump. The absorption heat pumps are mainly applying heat from Thisted Varmeforsynings halmforbrændingsanlæg (based on combustion of straw) or alternatively from garbage combustion (Dansk Fjernvarme 2019).

The production and injection wells are both vertical wells (Thi-2, -3). 200 m^3 water/hour can be produced from the production well with a wellhead at 1300 m depth. However, the production is typically < 150 m^3/hour (Carsten Møller, pers. comm., 2019). The plant has a capacity to supply to 2000 households after the second absorption heat pump was installed (Dansk Fjernvarme 2019). The plant is closed during the summer, from April to October.

The reservoir has a water temperature of 45°C (Vosgerau et al. 2015A). After cooling in the heat exchangers, the water is injected with a targeted temperature of *c.* 8°C, but actually up to 16°C (Mathiesen 2019).

Reservoir rock

The reservoir is the Upper Triassic–Lower Jurassic Gassum Formation, which was deposited under a humid climate in fluvial, lagoonal, tidal and shoreface depositional environments (Nielsen 2003).

The Gassum Formation in the Thisted area consists of quartz dominated (50–77 vol%) sandstones with common plagioclase (6–18 vol%) and K-feldspar (4–14 vol%). Some samples contain up to 23 vol% detrital clays of mainly illitic and kaolinitic composition (Weibel et al. 2017b). Rock fragments (max. 4 vol%) comprises sedimentary, plutonic, metamorphic and volcanic fragments. Mica (0–2 vol%) is mainly muscovite. Organic matter is present in up to 3 vol%. Heavy minerals (max 3 vol%) comprises mainly zircon, rutile and leucoxene-replaced Fe-Ti oxides). The major cementing phases are siderite (up to 22 vol%), calcite (up to 4 vol%), pyrite (up to 5 vol%), kaolinite (up to 3 vol%) and illitic clays (up to 1 vol%).

Porosity and permeability values up to 30% and 1500 mD respectively have been documented from core plug measurements (Weibel et al. 2017a).

Production problems

No problems during 30 years of operation.

The new injection well Thisted-5 showed from 2018 slightly decreased injectivity in the first months, probably due to fines migration caused by relatively higher flow rates than usually applied for this reservoir (Laier pers. comm. 2018).

3. Formation water chemistry

3.1 Sampling procedures

Solution compositions considered in the present study were measured by GEUS in 2017. Water samples from the three Danish geothermal plants were collected during operation to ensure representative samples. Samples for analysis of the chemical composition of the hot formation water were taken at the first possible position after the formation water had reached the surface. Thus, at Margretheholm and Sønderborg geothermal plants, sampling of the hot water was done at the top of the production well (A in figure 2.1 and 2.2, respectively), while at Thisted sampling was done just before the water entered the bag filter (A in figure 2.3). Sampling of the cooled formation water was done prior to injection of the water into the reservoir (C in Figure 2.1, and B in Figure 2.2. 2.3).

Sampling was facilitated through taps mounted in the production line at the geothermal plants. The brine was sampled into a beaker in which the pH and temperature were measured. Next, the brine was transferred to a 60 mL syringe, filtered through a 0.45 µm membrane filter and split into two separate polyethylene vials. Samples for analysis for cations received 1 vol% of 7M HNO_3 and were kept refrigerated until IC analysis (PerkinElmer Elan6100DRC Quadrupol) with a standard deviation of 3-15% depending on the element measured. Silicium, iron and trace elements were measured by ICP-MS (PerkinElmer Elan 6100DRC, Elan software version 3.3) with a detection limit of 0.001-5 mg/L depending on the element. Samples for anion analysis (chloride and sulphate) were frozen until ion-chromatography analysis (Metrohm IC, 819 detector, column Metrosep A sup. 5 – 150/4.0) with a quantification limit of 0.05 mg/L.

3.2 Chemical composition of the formation water

Solution compositions considered in the present study are presented in Table 3.1. The formation water at the three Danish geothermal plants are very saline with ionic strengths of c. 3.4 - 4. The quality of the measurements has been addressed by simple speciation calculations using PHREEQC 3.0 and its associated Pitzer database (Parkhurst and Appelo, 2013). These calculations indicate charge balance errors of up to -5.2% for the chemical analyses given in Table 3.1. Charge balances below 10% are generally accepted and the data from the three geothermal plants are therefore assumed to be very robust.

Table 3.1 Solution compositions at the production and injection wells at the three Danish geothermal plants.

	Margretheholm		Sønderborg		Thisted	
	Well head	After cooling	Well head	After cooling	Well head	After cooling
	A in Figure 2.1	C in Figure 2.1	A in Figure 2.2	B in Figure 2.2	A in Figure 2.3	B in Figure 2.3
Date	17-03-2017	17-03-2017	22-03-2017	22-03-2017	22-03-2017	22-03-2017
Temp. (°C)	72	20	46	15.9	43	15.6
pH	5.56	6.28	6.24	6.53	6.2	6.2
	(mg/L)	(mg/L)	(mg/L)	(mg/L)	(mg/L)	(mg/L)
HCO_3	29.7	30.6	60	62	45	45
Cl	133963	142600	97149	96228	98642	103000
Br	814	1150	219	222	314	430
SO_4	230	230	729	737	69	69
Na	53974	53800	55249	55443	51882	55000
Ca	20505	20400	3899	3918	6909	7500
Mg	2938	3020	1101	1093	1564	1600
Sr	724.85	780	193	198	370	340
K	636	550	219	218	248	270
Fe	0	15.1	6	12	8	29
Mn	16.75	19.2	6	6	15	13
Zn	3.67	3.9	0.14	0.51	1	0.12
Ba	17.28	19.7	0.8	0.7	18	13
Li	9.67	10.6				
Pb	0.55	0.38	0.01	0.006	0.01	0.02
Ni	0	0.25				
Cu	0	0.36				
Si	5.58	n.d.	5.65	4.6	4.65	4.93

To examine changes in the chemical composition of the brines and thus which chemical processes is likely to occur upon cooling of the formation waters at the three Danish geothermal plants, Schoeller diagrams (i.e. log concentrations) and the saturation state of the solutions with respect to relevant minerals are reported in Figure 3.1 – 3.3 for the three Danish geothermal plants. The saturation state of the brines with respect to selected minerals is indicated by the Saturation Index (SI) whereby positive and negative values indicate supersaturation and undersaturation, respectively.

For all three plants, concentrations of the aqueous species before and after cooling of the water are very similar (Figures 3.1 – 3.3). Nonetheless, the increase of the concentration in metallic elements (i.e. Fe, Zn etc.) at all three plants may reflect corrosion occurring between the well head and the heat exchanger. At Thisted, a large difference in the aqueous concentration of Zn in the formation water and the cooled formation water is observed, which may be due to precipitation of ZnS.

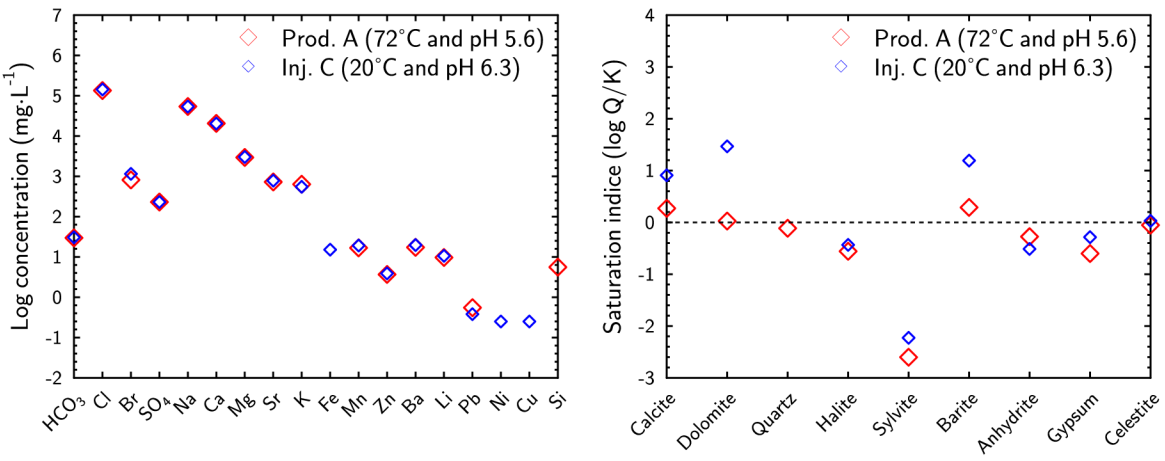

Figure 3.1: *Schoeller diagram and saturation indices of sampled fluids at the production and injection wells of the Margretheholm geothermal plant.*

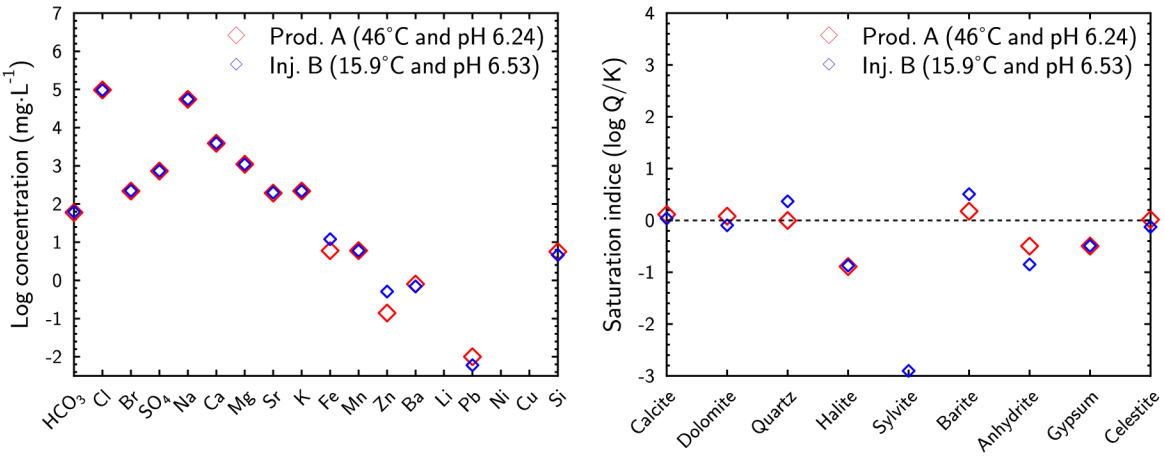

Figure 3.2: *Schoeller diagram and saturation indices of sampled fluids at the production and injection wells of the Sønderborg geothermal plant.*

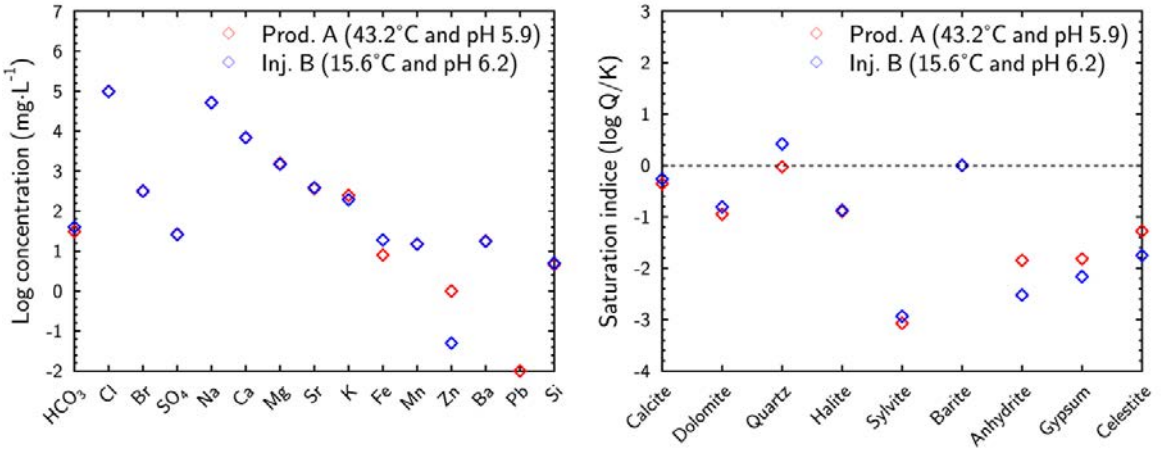

Figure 3.3: *Saturation indices of sampled fluids at the production and injection wells of the Thisted geothermal plant.*

The pore water of the geothermal reservoirs was assumed to be identical to the fluid sampled at the well head. At Margretheholm, saturation indices reported in Figure 3.1 indicates that the formation water (72 °C) is in equilibrium with calcite, dolomite, quartz, celestite and barite (i.e. log Q/K ~ 0, where Q is the ionic activity product and K the thermodynamic of the mineral considered). Equilibrium at different levels with sulphate minerals has been observed in the reservoir (Holmslykke et al., 2019). The barite is strongly supersaturated after heat extraction (i.e. log Q/K > 1.2) and may precipitate during and after cooling. Additionally, the supersaturation of carbonate minerals such as calcite and dolomite suggests CO_2 degassing during the sampling of the cooled formation water. This outgassing is thought to occur during the sampling rather than in the geothermal plant surface installations since a loss of pressure in the geothermal loop is not likely. The fluid cooling without CO_2 degassing destabilises carbonate minerals (i.e. thermodynamic behaviour). Therefore, precipitations of calcite and dolomite are not expected in the geothermal plant installations.

At Sønderborg, the formation water appears to be in equilibrium with respect to calcite, dolomite, quartz, barite and celestite (i.e. log Q/K ~ 0). Saturation indices of fluid recovered after the cooling highlights a possible precipitation of barite and quartz (i.e. log Q/K > 0). Such evolution agrees with the decrease of temperature that stabilises these minerals (e.g. Blanc et al., 2012). Nonetheless, the temperature difference before and after heat extraction (i.e. 46 and 15.9 °C) remains small and the reaction kinetics are clearly unfavourable for the quartz precipitation (e.g. Rimstidt and Barnes, 1980). Quartz precipitation can then reasonably be disregarded in predictive modelling. In contrast, the precipitation of barite is fast even at low temperature (e.g. Zhen-Wu et al., 2016); hence barite precipitation cannot be excluded during the fluid cooling down.

The pore water of the geothermal reservoir at Thisted appears to be at the equilibrium with respect to calcite, dolomite, barite and quartz. Saturation indices of fluid recovered after cooling of the brine highlight a potential for precipitation of barite (log Q/K > 0).

Thus, evaluation of the saturation state of the cooled formation water at the three Danish geothermal plants reveals that at all three plants there is a risk of barite precipitation.

4. Geochemical modelling

To further investigate the risk of scaling at the Danish geothermal plants, geochemical modelling has been performed to simulate the injection of the cooled formation water into the reservoir. The purpose of the modelling is to identify potential geochemical reactions (precipitation and/or dissolution) occurring in the reservoir upon reinjection of the cooled formation water. Precipitating minerals may clog the reservoir resulting in reduced injectivity, while dissolving processes may reduce the mechanical strength of the reservoir. Additionally, the possibility of barite nucleation in the injection wells has been checked. Thus, three different models have been conducted.

1. Modelling the injection of cooled formation water into the reservoir at Margrethehom and Sønderborg geothermal plants using MARTHE-PHREEQC code (Thiéry, 2015) and the pitzer database.
2. Modelling the injection of cooled formation water into the reservoir at all three geothermal plants using PHREEQC 3.0 (Parkhurst and Appelo, 2013) and the phreeqc database.
3. Modelling barite nucleation in the injection wells at all three geothermal plants using PHREEQC 3.0 (Parkhurst and Appelo, 2013) and the pitzer database.

For comparison, the injection of the cooled formation water into the reservoir has been modelled using two different approaches. Trémosa et al. (2014) have demonstrated that calculations using the B-dot model, an extension of the Debye-Hückel activity model, failed in reproducing simple mineral solubilities for NaCl salinities higher than 1 mol kg_w^{-1} even though the saline waters are of NaCl type. In contrast, calculations using the Pitzer interaction model clearly improved experimental data reproduction and allowed mineral solubility to be captured as a function of salinity in a relatively good manner. Therefore, considering the salinities of the geothermal reservoirs, the Pitzer thermodynamic database released with the PHREEQC code is the more appropriate database to use in this study and is used in model 1) above. However, numerous elements are not available in the pitzer database (e.g. Al, Fe(3), S(-2) etc.), leading to non-negligible limitations in the study of saline solutions (Lach et al., 2018; Lassin et al., 2018). Several minerals were not considered in MARTHE-PHREEQC modelling (e.g. Al bearing mineral or redox sensitive phases). Therefore, to address the possibility of dissolution and precipitation of these solid phases upon injection of the cooled formation water, a phreeqc.dat database was used (model 2) above). Phreeqc.dat is based on Debye-Hückel theory, which provides the most accurate results for low-saline solutions. With increasing ionic strength, the certainty of the results decreases. To check the possible discrepancies caused by execution of the models using Debye-Hückel theory instead of Pitzer equations for the solutions at Sønderborg, Margretheholm and Thisted, we have calculated and compared saturation indices of the key solid phases using both, *phreeqc.dat* and *pitzer.dat*. prior to the run of transport models.

Database (thermodynamic and kinetic), geometry, transport properties (e.g. flow rate, porosity etc.) considered here provide numerical results as realistic as possible. Nonetheless, several processes such as the formation of biofilm, corrosion processes and transport of parti-

cles have not been taken into account because of lack of data reported in the model databases and current software capabilities (e.g. transport of eroded particles). Therefore, the numerical results have some inherent limitations.

4.1 Model description

4.1.1 MARTHE-PHREEQC

MARTHE-PHREEQC reactive transport modelling software is an extension of MARTHE software (http://marthe.brgm.fr/ Thiéry, 2015), which has been upgraded by coupling with the PHREEQC chemical module (Parkhurst and Appelo, 2013). The coupling algorithm is purely sequential; at each time step, MARTHE computes the hydraulic head field and hence the velocity in the entire domain. It then transports all considered dissolved chemical elements and also transports heat to determine the temperature field on which the geochemical reactions depend. Then, the geochemistry is computed using the PHREEQC module in each model cell.

A single-layer homogeneous model was applied to simulate the geothermal reservoirs of Sønderborg and Margretheholm (Figure 4.1). The mesh was radial type with X, Y, and Z coordinates coinciding with the radius, angle, and layer of the model, respectively. A homogeneous porosity was assumed in the geological formation and, similarly to the reservoir thickness, depends on the considered location (i.e. Sønderborg or Margretheholm). A mesh size of 2.5 cm was considered close to the injection well and increases progressively up to 20 m with distance. The model assumed upper and lower impervious walls following the approximate analytical solution of Vinsome and Westerveld (1980) (thermal conduction perpendicular to the aquifer) implemented in MARTHE. This analytical solution which avoids the vertical discretization of the clay layers considerably reduces the number of meshes in the model, thereby decreases the computation time.

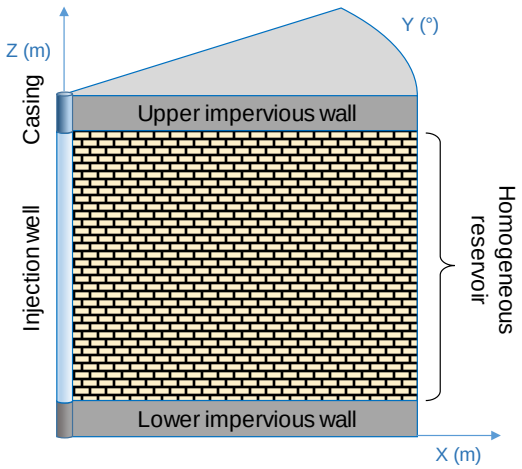

Figure 4.1: *Schematic representations of geometry applied to simulate the geothermal reservoirs of Sønderborg and Margretheholm with MARTHE-PHREEQC.*

Simulations considered the recorded flow rate at the geothermal plants. Evolutions over time are reported in Figure 4.2. The total durations of simulations were 4.6 and 10.6 years for Sønderborg and Margretheholm, respectively. Time steps for calculations were a function of flow rates and were imposed as small as possible:

- min = 2.6 seconds at 169 m^3 h^{-1} and max = 1 day at 0 m^3 h^{-1} for Sønderborg;
- min = 13.3 seconds at 241 m^3 h^{-1} and max = 1 day at 0 m^3 h^{-1} for Margretheholm.

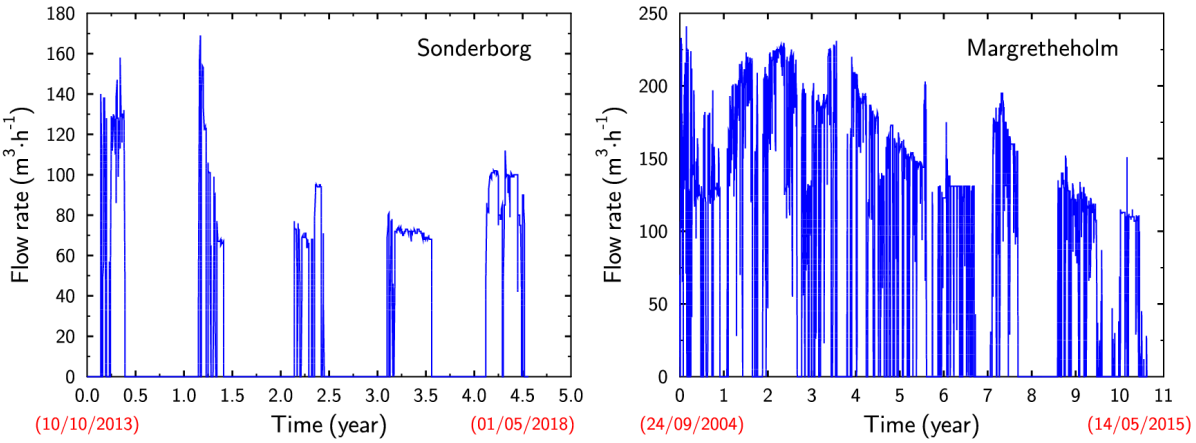

Figure 4.2: *Evolutions of flow rates recorded at the Sønderborg and Margretheholm geothermal plants and used as input in the MARTHE-PHREEQC modelling.*

The general parameters used for the simulations were defined using data from scientific literature and are summarised in Table 4.1. The chemical composition of the brines used for the modelling are shown in Table 3.1.

Table 4.1: General parameters used for the simulations used as input in the MARTHE-PHREEQC modelling.

Simulation parameters	**Values**
Initial temperature (°C)	49 (Sønderborg) 72 (Margretheholm)
Molecular diffusion (m^2 s^{-1})	1.5 x 10^{-10}
Volumetric heat capacity of minerals (J m^{-3} °C^{-1})	2 x10^6
Heat capacity of the water (J kg^{-1} °C^{-1})	4185
Thermal conductivities of minerals (W m^{-1} °C^{-1})	2.5
Thermal conductivities of water (W m^{-1} °C^{-1})	0.6

Mineralogical composition of the reservoir sandstones is defined from Mineralscan of cuttings samples (Olivarius et al. 2019). Simplified solid chemistry calculated from the mineral scans made by SEM is reported in **Fejl! Henvisningskilde ikke fundet.** and 4.3. Due to the limited range of minerals in the Pitzer database, a large fraction of minerals (e.g. feldspar, albite and muscovite) were considered as unreactive phases. Nonetheless, from a kinetic point of view, these simplifications mainly concern mineral phases that are less likely to precipitate (e.g. Palandri and Kharaka, 2004).

The porosity was estimated from petrophysical logs to be of 22% at Margretheholm and 28% at Sønderborg. In the calculation of simplified solid chemistry we used the porosity of 20% and 30% for Margaretholm and Sønderborg, respectively (Table 4.2. and 4.3.).

Table 4.2: Simplified solid chemistry considered for the Margretheholm geothermal reservoir used as input in the MARTHE-PHREEQC modelling..

Name in PITZER.DAT (Parkhurst and Appelo, 2013)	**Mass fraction**	**mol L^{-1} of solution***	**mol L^{-1} of rock***
Calcite	0.0355	3.760	0.752
Dolomite	0.0684	3.931	0.786
Quartz	0.5639	99.397	19.879
Unreactive	0.3321	13.528	2.706

**calculated assuming a porosity of 20%.*

Table 4.3: Simplified solid chemistry the Sønderborg geothermal reservoir used as input in the MARTHE-PHREEQC modelling..

Name in PITZER.DAT (Parkhurst and Appelo, 2013)	**Mass fraction**	**mol L^{-1} of solution***	**mol L^{-1} of rock***
Calcite	0.0507	3.096	0.929
Dolomite	0.0002	0.005	0.002
Quartz	0.3311	33.700	10.110
Unreactive	0.6181	14.540	4.362

**calculated assuming a porosity of 30%.*

Barite precipitation is simulated using a kinetic law based on the TST (transition state theory, Lasaga, 1981). Kinetic parameters have been extracted from Zhen-Wu et al. (2016). Other minerals considered have been processed at local equilibrium. Basic lines for the consideration of barite kinetics in PHREEQC are given below:

```
Barite # from Zhen-Wu et al. (2016)
-start
10 mole = 0
20 If (m <= 0) and (SR("Barite") < 1) Then GoTo 100
30 S = 2E-5 # Fitted value to limit the clogging of the Magretheholm well (in agreement with injected flow rate)
40 Mm = 233.389 # molar mass in g/mol
50 k = 1.4e-3 * exp(-25000/(8.314*TK)) * 10^(0.6*sqrt(mu)) # suppressing of pH dependence as there is no significant effect in Zhen-Wu et al. (2016): * (ACT("H+")^0.03)
60 If (SR("Barite") > 1) Then n = 1 else n = 0.2
70 rate = S * m * Mm * k * (1 - SR("Barite")^n)
80 If (m <= 0) and (SR("Barite") > 1) then rate = -1E-10 # nucleation of barite when mineral is not present
90 mole = rate * Time
100 Save mole
-end
```

The surface areas (S in line 30) is adjusted to limit the formation of barite, and therefore the porosity clogging, in the Margretheholm geothermal reservoir in agreement with injected flow rates during 10.6 years.

4.1.2 PHREEQC 3.0

1D reactive transport modelling of injection of cooled brines into the geothermal reservoirs was conducted simulating a 1-kilometer-long column at Sønderborg and Margretheholm. The cooled brine at Thisted progressed to a distance of more than 1 km from the injection well, thus a 1.5-km-long column was implemented in the model for Thisted. The columns were divided into 5-m-long cells, which resulted in 200 cells at Sønderborg and Margretheholm and 300 cells at Thisted.

Injected solutions in the numerical simulations (Table 3.1) were equilibrated with calcite and dolomite at all three geothermal plants. Aqueous solutions in the reservoirs were equilibrated with solid phases, for which the formation water showed supersaturation or equilibrium state (barite and celestite) (Figures 3.1 – 3.3) and with solid phases present in the reservoirs (albite, K-mica, quartz, K-feldspar, kaolinite, illite, chlorite, calcite and dolomite). Initial amounts of the minerals present in the reservoirs were calculated based on the results of mineral scans made by SEM (Tables 4.4 – 4.6). Due to the conditions in the reservoirs dissolution of albite, K-mica and quartz is unlikely. Thus, only precipitation of these phases was allowed in the model. For the remaining phases both precipitation and dissolution could occur. Barite precipitation/dissolution which is considered the most likely to occur at the described geothermal plants was modelled using kinetic rates after Zehn-Wu et al. (2016).

Table 4.4: Extended solid chemistry in the Margretheholm geothermal reservoir used as input in the PHREEQC modelling.

Name in PHREEQC.DAT (Parkhurst and Appelo, 2013)	Mass fraction (%)	mol L^{-1} of solution*
Albite	5.28	1.25
Calcite	3.1	1.92
Chlorite	6.25	0.7
Dolomite	2.41	0.808
Illite	0.02	0.003
Kaolinite	0.1	0.02
K-feldspar	19.98	4.44
K-mica	0.62	0.1
Quartz	49.19	50.62

Table 4.5: Extended solid chemistry in the Sønderborg geothermal reservoir used as input in the PHREEQC modelling.

Name in PHREEQC.DAT (Parkhurst and Appelo, 2013)	Mass fraction (%)	mol L^{-1} of solution*
Albite	0.6	0.14
Calcite	3.2	1.98
Chlorite	2.4	0.27
Dolomite	0.01	0.003
Illite	0.01	0.002
Kaolinite	0.6	0.15
K-feldspar	1.3	0.29
K-mica	8.3	1.29
Quartz	20.9	21.52

Table 4.6: Extended solid chemistry in the Thisted geothermal reservoir used as input in the PHREEQC modelling.

Name in PHREEQC.DAT (Parkhurst and Appelo, 2013)	Mass fraction (%)	mol L^{-1} of solution*
Albite	17.79	4.19
Calcite	0.01	0.01
Chlorite	5.03	0.56
Dolomite	0	0
Illite	0	0
Kaolinite	3.15	0.75
K-feldspar	12.39	2.75
K-mica	1.56	0.24
Quartz	52.2	53.72

Pressures in the reservoirs were set to 121, 132 and 260.4 bar for Sønderborg, Margretheholm and Thisted, respectively. In order to maintain the temperature gradient in the models representing the gradient around the injection well, the REACTION_TEMPERATURE mod-

ule in PHREEQC 3.0 was used, assigning fixed temperatures along the 1D columns in accordance with the temperatures observed in the reservoirs during operation of the geothermal plants. Applied temperature gradients are shown in Figure 4.3.

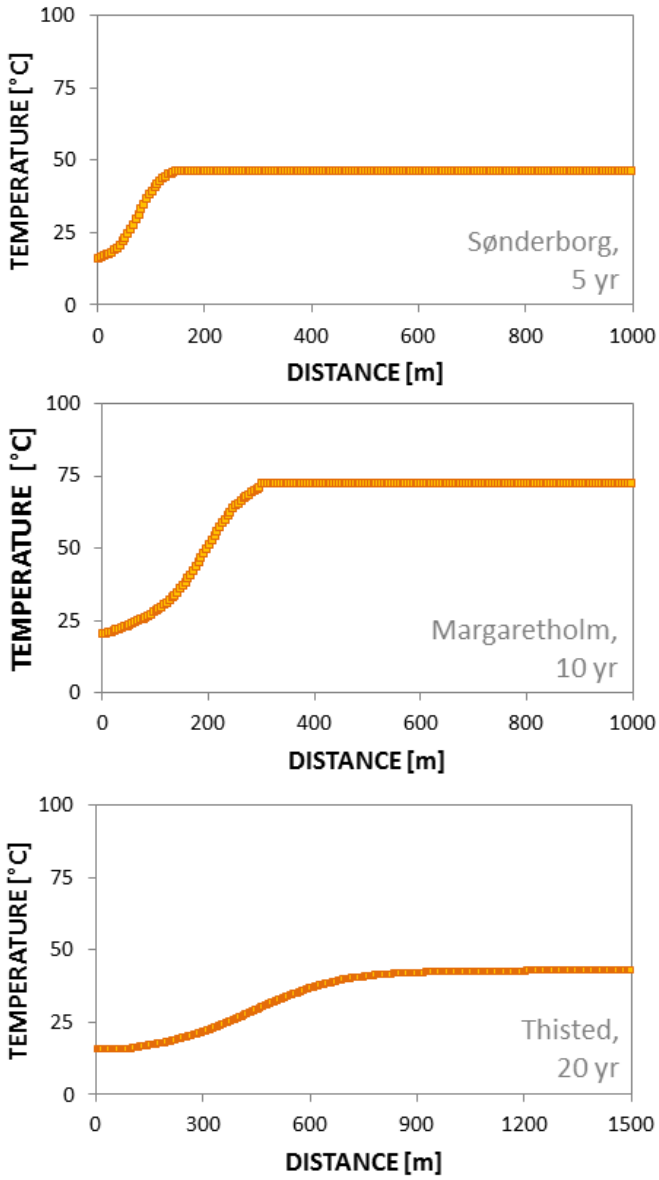

Figure 4.3: *Temperature gradients used in the 1D simulations of inflow of the cooled brines into the geothermal reservoirs.*

The models were run for 5, 10 and 20 years for Sønderborg, Margretheholm and Thisted, respectively. Injection rates differed between 70–130 m^3/d at Sønderborg and were set as an average fixed value of 150 m^3/d at Margretheholm and 110 m^3/d at Thisted. Reservoir porosity equaled 0.3 at Sønderborg, 0.2 at Margretheholm and 0.25 at Thisted. Schematic set up of the 1D transport models in the reservoir is presented in Figure 4.4.

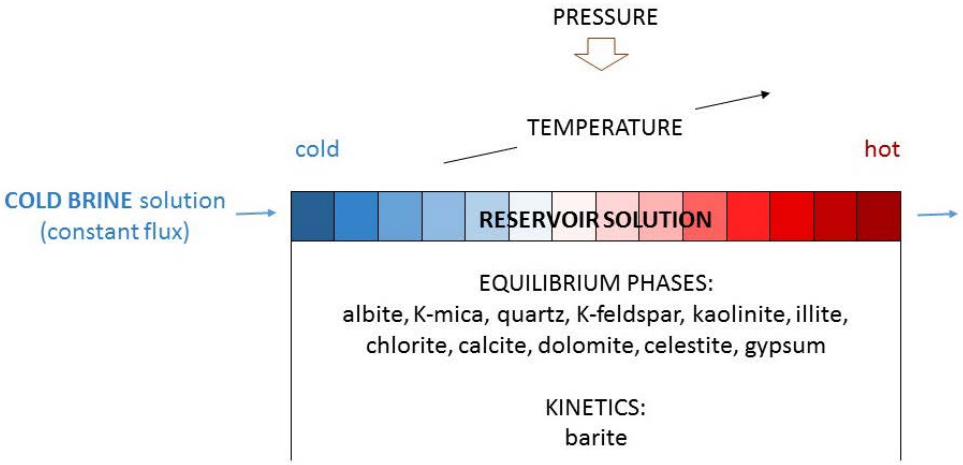

Figure 4.4: *Scheme of the 1D transport models of the injected brine through the reservoir.*

4.1.3 Barite nucleation in wells

Barite nucleation in the injection wells at Thisted, Margretheholm and Sønderborg was modelled using the 1D barite nucleation model developed in PHREEQC 3.0 (Parkhurst and Appelo, 2013) by Diederiksen et al. (in prep.):

```
Nucleation
-start
2 A = 2.0e-3
3 R = 8.314462
4 Ea = 24000
5 nH = 0.03
6 nI = 0.6
7 n = 1
10 V_BaSO4 = 0.0862 #nm3/molecule
11 Kb = 1.38E-23
12 Ns = 5.3E16 # number of sites for nucleation
13  LGY  =  -1*1*A*exp(-Ea/(R*(TK)))*act("H+")^nH*10^(nI*sqrt(mu))*(1-
(SR("Barite"))^n) * 0.0000519 * 31536000  * 1e9 #LGY is the linear growth
rate in nm per year
14 LGS = LGY / 31536000 # linear growth rate in nm/s
15 PUT(LGS,42)
16 pi = 3.14
20 k = GET(41) # l = CELL_NO
50 T_I =  0.02 * 31536000 ##########CHANGE parm(2) * 31536000  # making
parm 2 from years to seconds
51 PUT(T_I, 30)
60 l = GET(40)
61 s = 0.02  #####CHANGE
140 Gamma_CW = 3e-19#3e-19 # j/nm2 (3e-19: Jang et al., 2003)
141 Gamma_SW = 7.9e-19 # j/nm2 (7.9e-19 #Magnetite, Navrotsky et al.,
2010)
142 Gamma_CS = 2.4e-19 # j/nm2
```

```
####################
150 Gamma_mark = (-0.05 * TC + 9.0)*1e-20 #(-0.1 * TC + 12.5)*1e-20
#3.9e-20 # 3.1  Gamma_CW * (1 - ((Gamma_SW-Gamma_CS)/(2 * Gamma_CW)))
####################
152 Zel = 1e-3
160 Delta_G_nuc =  (8 * pi * Gamma_mark^3 * V_BaSO4^2)/(3 * ((TK * Kb *
LOG(SR("Barite"))))^2)  #  Delta_G_nuc  =   (8  *  pi  *  Gamma_mark^3  *
V_BaSO4^2)/(3 * ((TK * Kb * LOG(SR("Barite"))))^2)
170 A_nucl = Ns * LGS * Zel / 0.55
180 J_nucl = A_nucl * exp (-1*Delta_G_nuc/(Kb *(TK)))
202 PUT(LGS,1,l,k)
203 PUT(J_nucl, 2,l,k)
204 A_tot = GET(50,l,k)
205 If A_tot < s * 1e18 THEN GOTO 900 ELSE A_tot = 1e18 * s #
207 GOTO 2002
INCLUDE$ C:/Users/jka/Desktop/Nucl_KD_new_4pi
2002 PUT(A_tot, 50,l,k)
2300 save A_tot
-end
```

The model is based on a Pitzer database extended by Diederiksen et al. (in prep.) and kinetic rates described in Zhen-Wu et al. (2016). Each of the injection wells was divided into 10 cells of an equal length. Density of the sites available for barite nucleation at the wells was dependent on the well diameter. At all wells, the model was run for one week of an operation. Injection rates used in the model equaled 150, 130 and 110 m^3/h for Margretheholm, Thisted and Sønderborg respectively. A linear pressure gradient was assumed at each of the wells. Pressure equaled 10 bar at the well head for all wells and at the well bottom: 145 bar in Sønderborg, 165 bar in Thisted, 310 bar in Margretheholm. Transported solutions had temperature and composition of the cold brines described in Table 3.1. The conceptual model of barite nucleation is showed in Figure 4.5.

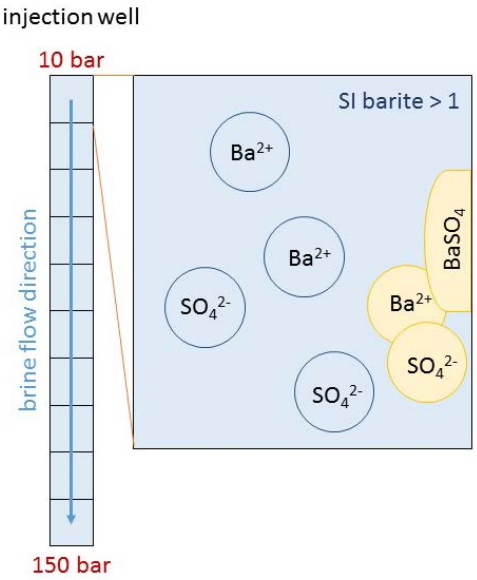

Figure 4.5: *Conceptual model of barite nucleation in the injection wells. SI is a saturation index of a brine with respect to barite and its value has to exceed 1, in order for a barite nucleation to occur (Diederiksen et al., in prep.).*

5. Results and discussion

5.1 Reactive surface area

To estimate the reactive surface area of barite in the reservoir, a sensitivity analysis has been carried out by increasing the surface from 10^{-5} to $5x10^{-5}$ m^2 g^{-1} using the data for Margretheholm geothermal plant. The amount of sulphate minerals and resulting porosity (i.e. volume balance) modelled after 10.6 years are reported on Figure 5.1. The amount of precipitated barite is very sensitive to the considered surface area.

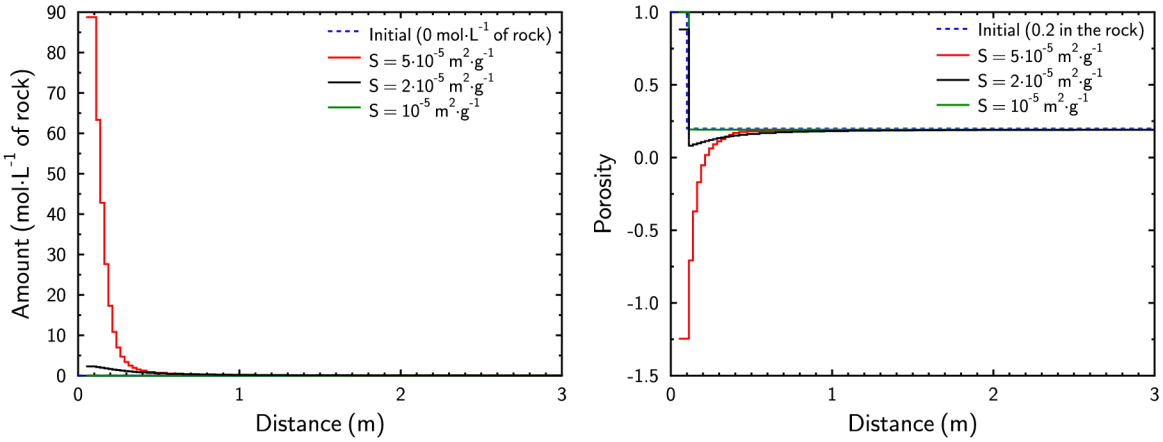

Figure 5.1*: Amount of precipitated barite and resulting porosity (i.e. volume balance) calculated after 10.6 years for the Margretheholm geothermal plant as function of the considered reactive surface area.*

It clearly appears that a reactive surface of 5 10^{-5} m^2 g^{-1} leads to an over estimation of the precipitated amount of barite. Indeed, after 10.6 years of water-rock interactions, the mineral formation lead to a massive clogging of the porosity in the near field of the injection well (Figure 5.1). Such result disagrees with recorded flow rates during the considered operating period (Figure 4.2). Note that the porosity calculation is based on a simple volume balance and therefore, can lead to negative values. In contrast, reactive surface areas of 2 10^{-5} and 10^{-5} m^2 g^{-1} appear to be more realistic (Figure 5.1) and are compatible with flow rates reported on Figure 4.2. Nonetheless, formation of barite is almost totally inhibited considering 10^{-5} m^2 g^{-1} and therefore, a reactive surface area of 2 10^{-5} m^2 g^{-1} is considered in this study.

5.2 MARTHE-PHREEQC

5.2.1 Margretheholm geothermal reservoir

Mineralogical evolutions calculated for the Margretheholm geothermal reservoir using the MARTHE_PHREEQC model with the pitzer database are reported in Figure 5.2 (calcite and dolomite) and Figure 5.3 (barite and celestite).

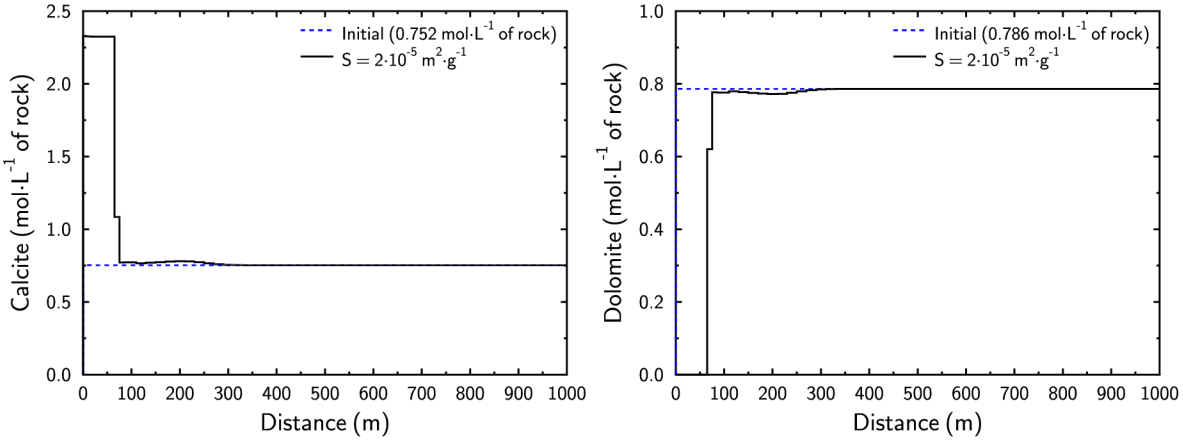

Figure 5.2: *Amounts of calcite and dolomite calculated after 10.6 years for the Margretheholm geothermal plant.*

Numerical results indicate a conversion of dolomite into calcite (Figure 5.2). Dolomite/ankerite conversion (approximately equivalent to dolomite/calcite conversion) has been currently observed in experiments (Debure et al., 2017; Gysi and Stefánsson, 2012); thus, a similar process could be expected in the geothermal reservoir. Nonetheless, carbonate minerals have been processed at local equilibrium (i.e. no kinetics) and the magnitude of mineralogical evolution is probably overestimated by the model. Even if such a process is important for oil reservoirs (e.g. Rodríguez-Morillas et al., 2013), its effect on resulting porosity in the framework of the Margretheholm geothermal plant is negligible compared to the precipitation of sulphate bearing minerals (Figure 5.12).

The barite (under kinetic control) and celestite (processed at local equilibrium) are expected to precipitate in the near field of the injection well (Figure 5.3). The salt formation is essentially promoted by the cooling of fluid after heat extraction (i.e. decreasing of solubility with the decrease of temperature). Such formation may affect the injection of cooled water by scaling (i.e. permeability damage caused by barite deposits) directly in pipe or by clogging the porosity of the reservoir rock. The mineral is one of the common scales in oil production (e.g. Oliveira et al., 2019) and in geothermal plant installation (e.g. Bozau et al., 2015). The porosity profile simulated for the Margretheholm geothermal plant mainly decreases due to the precipitation of barite (Figure 5.4**:**). Due to this porosity reduction, the injection pressure would be increased to maintain a constant flow rate. Unfortunately, MARTHE-PHREEQC is

currently not able to process feedback of mineralogical transformations on transport properties (i.e. evolution of permeability) and therefore, the increase of injection pressure was not calculated.

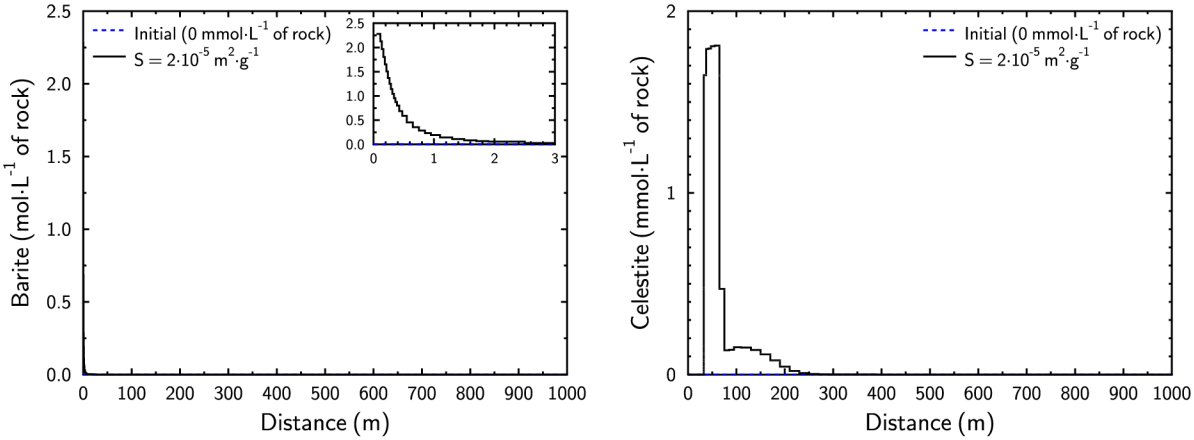

Figure 5.3*: Amounts of barite and celestite calculated after 10.6 years for the Margretheholm geothermal plant.*

After 10.6 years of geothermal production, the numerical modelling indicates that a decrease of temperature at the production well is unlikely, which agrees with recorded data. The cold injection front progresses up to 300 m, which is less than the distance between the injection and production wells (i.e. 1300 m). A thermal breakthrough (i.e. when the progression front of the cold bubble reaches the production well) is not predicted, explaining the efficiency of geothermal production during the operating period.

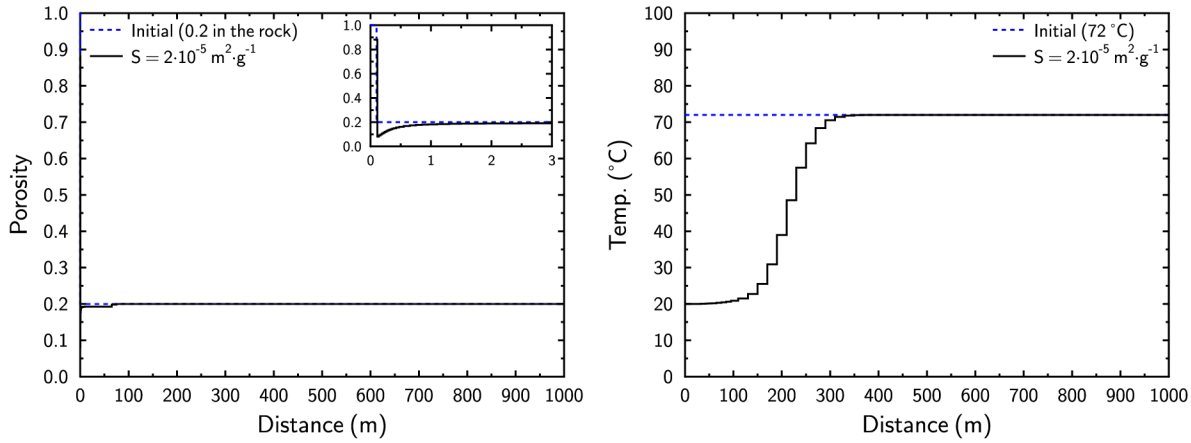

Figure 5.4: *Porosity and temperature profile calculated after 10.6 years for the Margretheholm geothermal plant.*

Similarly to barite, and from a thermodynamic point of view, a decrease of temperature stabilises the quartz, a primary mineral. Nonetheless, the precipitation kinetics of quartz is insignificant at the injected temperature (i.e. 20 °C) and quartz formation can be disregarded considering the investigated period (i.e. 10.6 years). Therefore, the quartz precipitation has been inhibited in the present modelling. In contrast, a potential formation of amorphous silica has been considered. Nonetheless, amorphous silica phase remains undersaturated during the whole duration of the modelling.

Thus, the modelling indicates that both barite and celestite are expected to precipitate in the reservoir at Margretheholm in significant amounts. Precipitation of celestite is expected to occur c. 50-100m from the injection well, whereas barite precipitation is likely to occur immediately upon injection into the reservoir. According to the model, both processes may reduce the porosity, however, particularly precipitation of barite near the injection well may reduce the reservoir porosity significantly (Figures 5.3 and 5.4) and may probably also reduce the injectivity of the reservoir.

5.2.2 Sønderborg geothermal reservoir

Evolutions of calcite and dolomite modelled in the geothermal reservoir of the Sønderborg plant after 4.6 years of operating period are reported in Figure 5.5. A conversion of dolomite into calcite is also modelled. Nonetheless, the initial amount of dolomite inside the rock formation is low and such process can be clearly neglected.

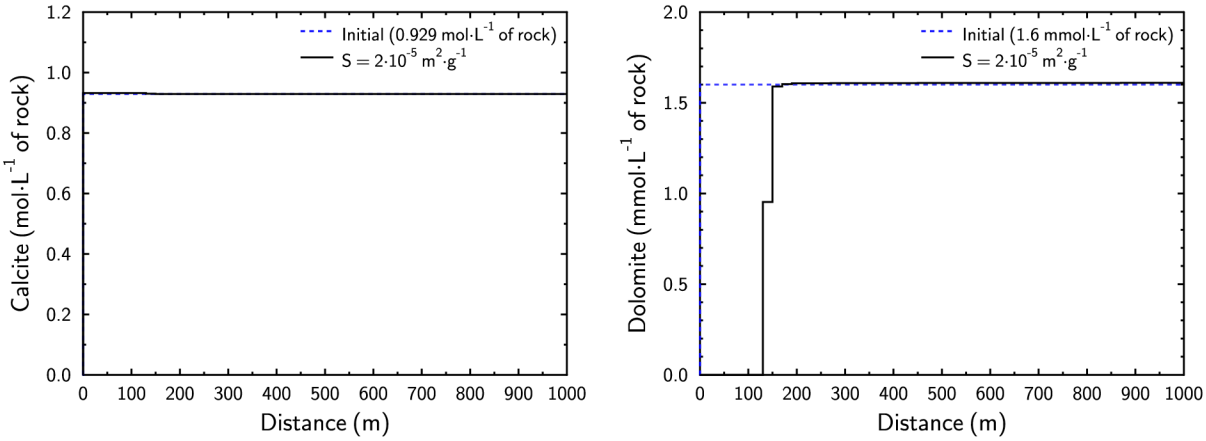

Figure 5.5: *Amounts of calcite and dolomite calculated after 4.6 years for the Sønderborg geothermal plant.*

The precipitated amounts of barite and celestite are low (Figure 5.6). The change in porosity resulting from mineralogical transformations is insignificant (Figure 5.7). The cold injection front progresses up to 175 m that is in agreement with the short operating period considered here (i.e. 4.6 years) and temperatures recorded at the production well. The progression is shorter than the well head distance (i.e. 760 m).

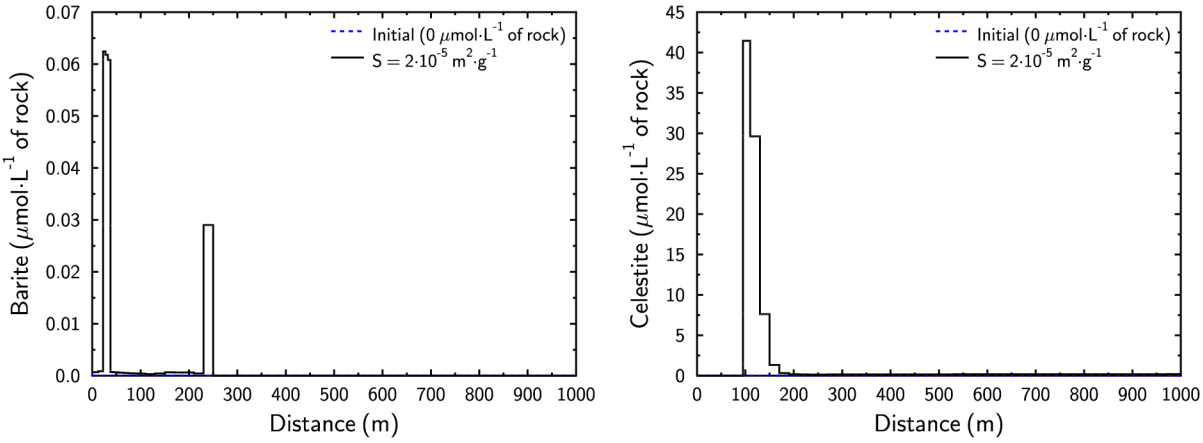

Figure 5.6: *Amounts of barite and celestite calculated after 4.6 years for the Sønderborg geothermal plant.*

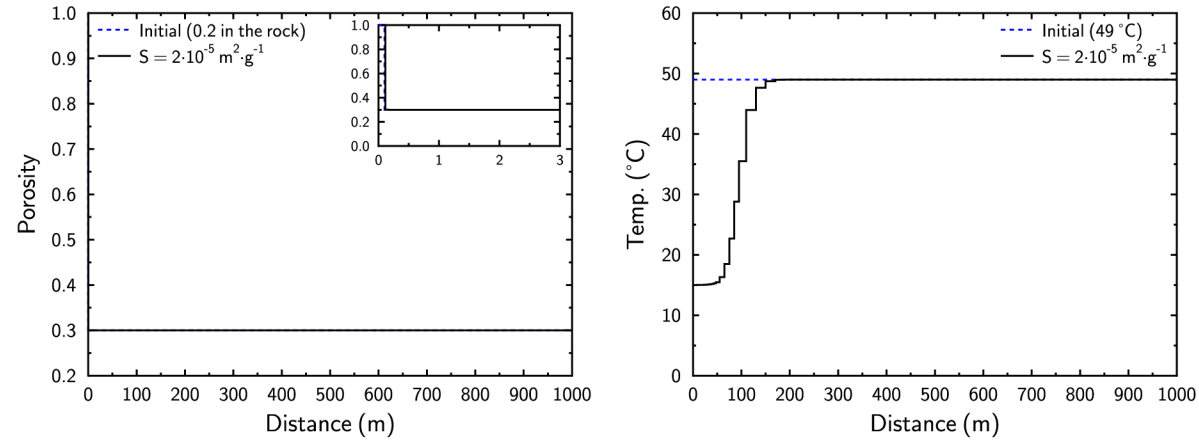

Figure 5.7: *Porosity and temperature profile calculated after 4.6 years for the Sønderborg geothermal plant.*

5.3 PHREEQC 3.0

Results of the numerical calculations with the PHREEQC model in the studied geothermal reservoirs are presented in Figures 5.8 (calcite and dolomite), 5.9 (barite) and 5.10, 5.11 and 5.12 (Al-bearing minerals).

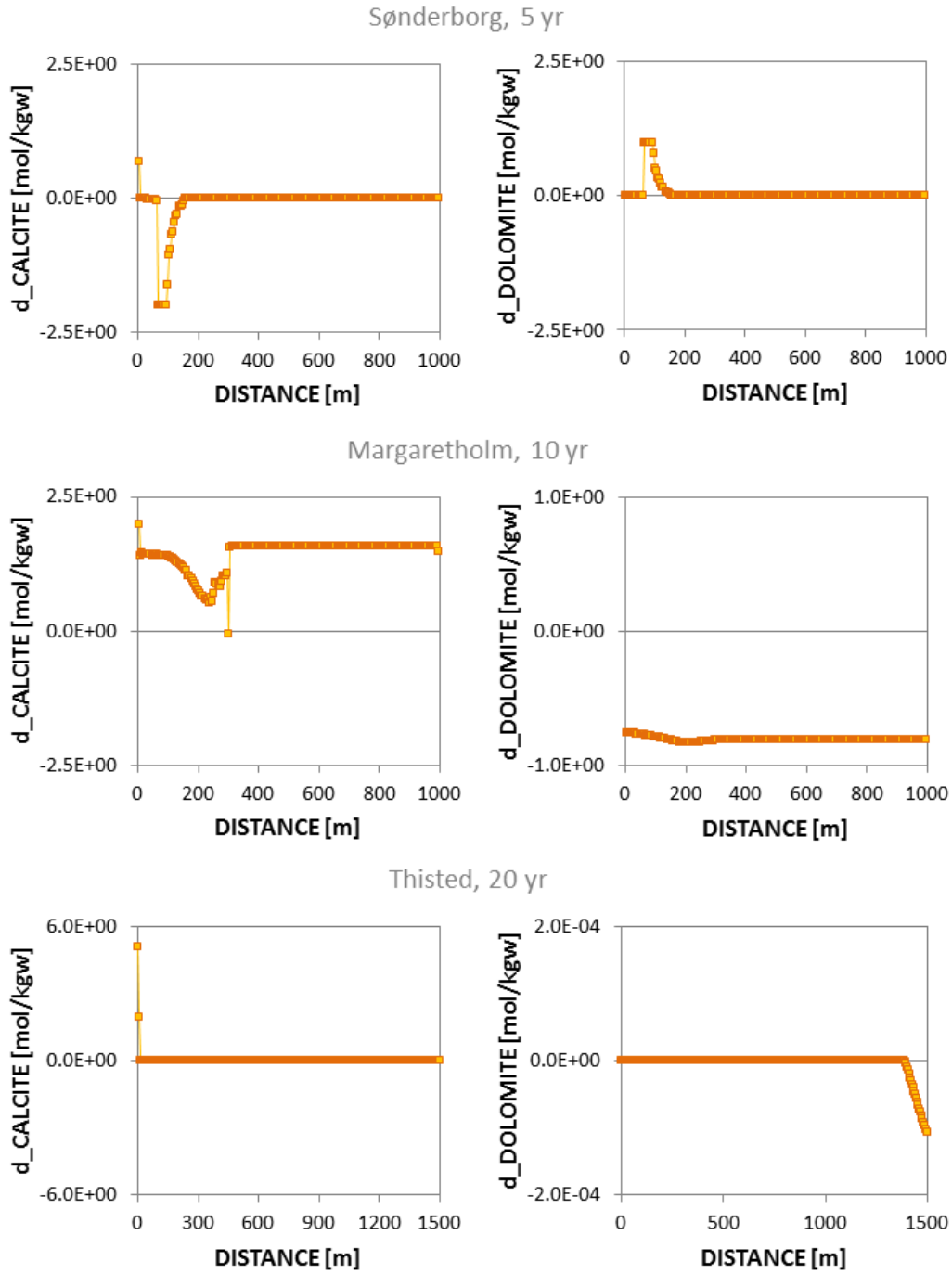

Figure 5.8: *Amounts of calcite and dolomite calculated for the geothermal reservoirs after 5 (Sønderborg), 10 (Margaretholm) and 20 (Thisted) years of operation of the geothermal plants. Mineral precipitation and dissolution are indicated by positive and negative values, respectively.*

Similarly, to the MARTHE-PHREEQC models, the PHREEQC calculations indicate conversion of dolomite into calcite and vice versa (Figure 5.8). However, the results of the PHREEQC calculations partially show an opposite mineral transformation than MARTHE-

PHREEQC models. It is probably due to the discrepancies between applied databases. While pitzer.dat database indicates in most of the cases supersaturation of the solutions with respect to calcite, calculations performed using phreeqc.dat database indicate slight sub saturation with respect to calcite. Another important factor influencing equilibrium conditions between calcite and dolomite is temperature distribution, which in the simple PHREEQC calculations was assumed to be at fixed values in each of the cells (Figure 4.4), while in MARTHE-PHREEQC models the temperature front migrated with time into the reservoir. At the geothermal reservoir at Thisted there is no transformation between calcite and dolomite, and calcite precipitation is likely to occur near the injection well, while dolomite dissolution takes place further in the reservoir, at the temperatures above 43 °C. As indicated in the MARTHE-PHREEQC models, transformations between calcite and dolomite do not have an important influence on the reservoir porosity and performance of the geothermal plants.

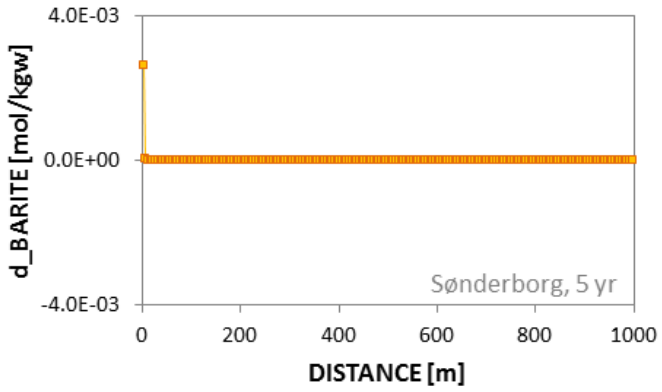

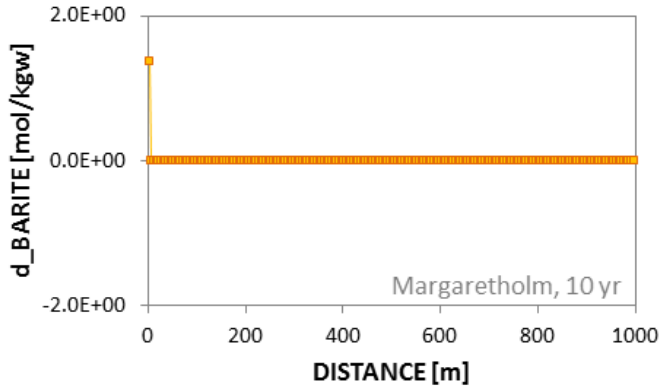

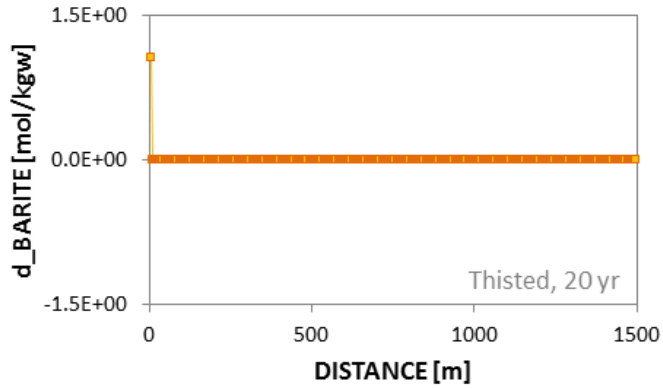

Figure 5.9: *Amounts of barite calculated for the geothermal plants. Mineral precipitation and dissolution are indicated by positive and negative values, respectively.*

More important is barite precipitation, which takes place in the proximity of the injection wells. The amounts of barite precipitated at each of the geothermal reservoirs are presented in Figure 5.9. Assuming a flow rate of 150 m^3/h, 130 m^3/h and 110 m^3/h for Margretheholm, Sønderborg and Thisted, respectively, the barite production amounts to c. 1.1 g/h, 0.01 g/h and 0.46 g/h for Margretheholm, Sønderborg and Thisted, respectively. These results are consistent with the output from the MARTHE-PHREEQC models showing that barite precipitation may affect the porosity at Margretheholm whereas barite precipitation is insignificant at Sønderborg.

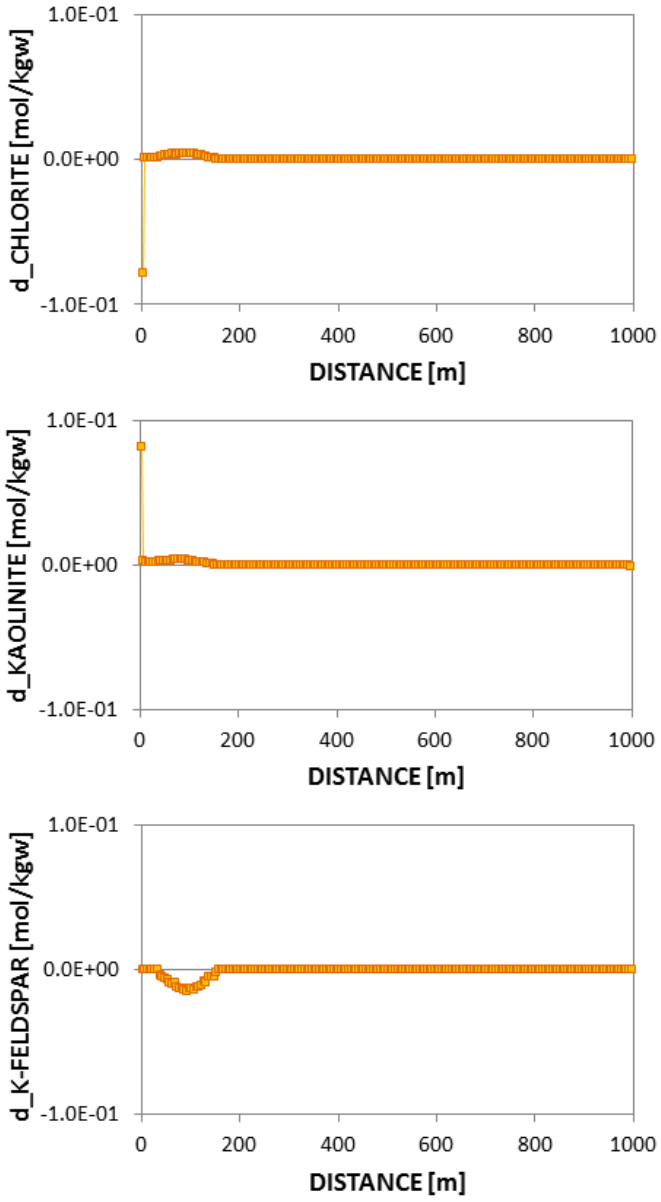

Figure 5.10: *Amounts of chlorite, kaolinite and K-feldspar calculated for Sønderborg geothermal reservoir after 5 years of plant operation. Mineral precipitation and dissolution are indicated by positive and negative values, respectively.*

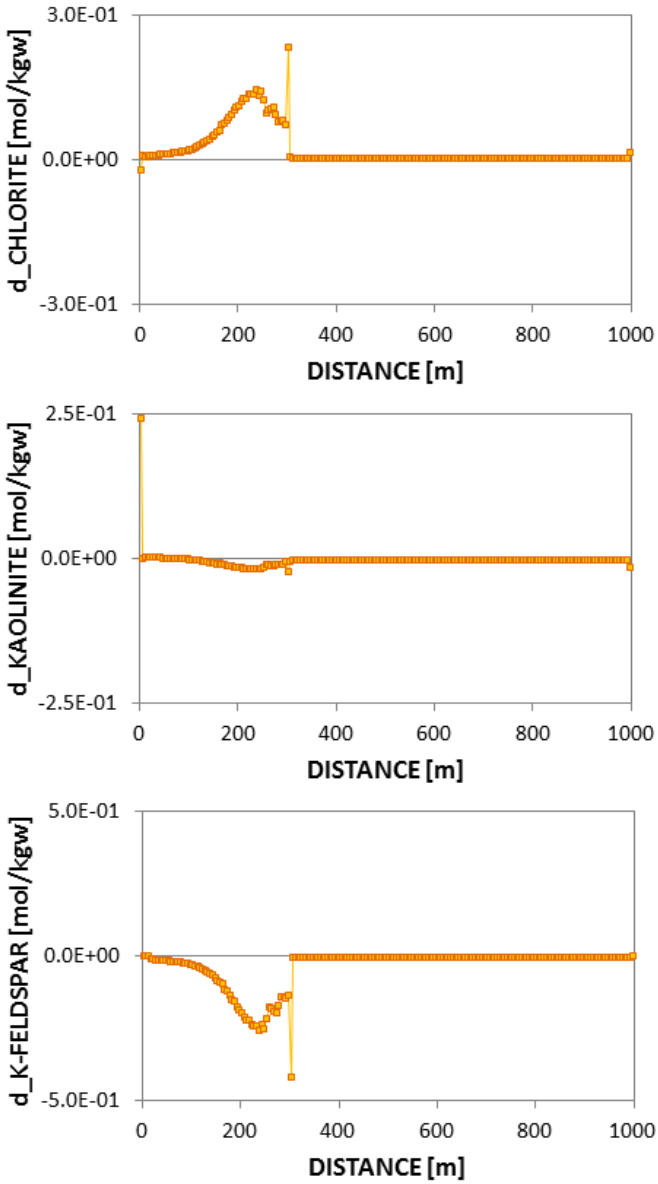

Figure 5.11: *Amounts of chlorite, kaolinite and K-feldspar and calculated for Margretheholm geothermal reservoir after 10 years of plant operation. Mineral precipitation and dissolution are indicated by positive and negative values, respectively.*

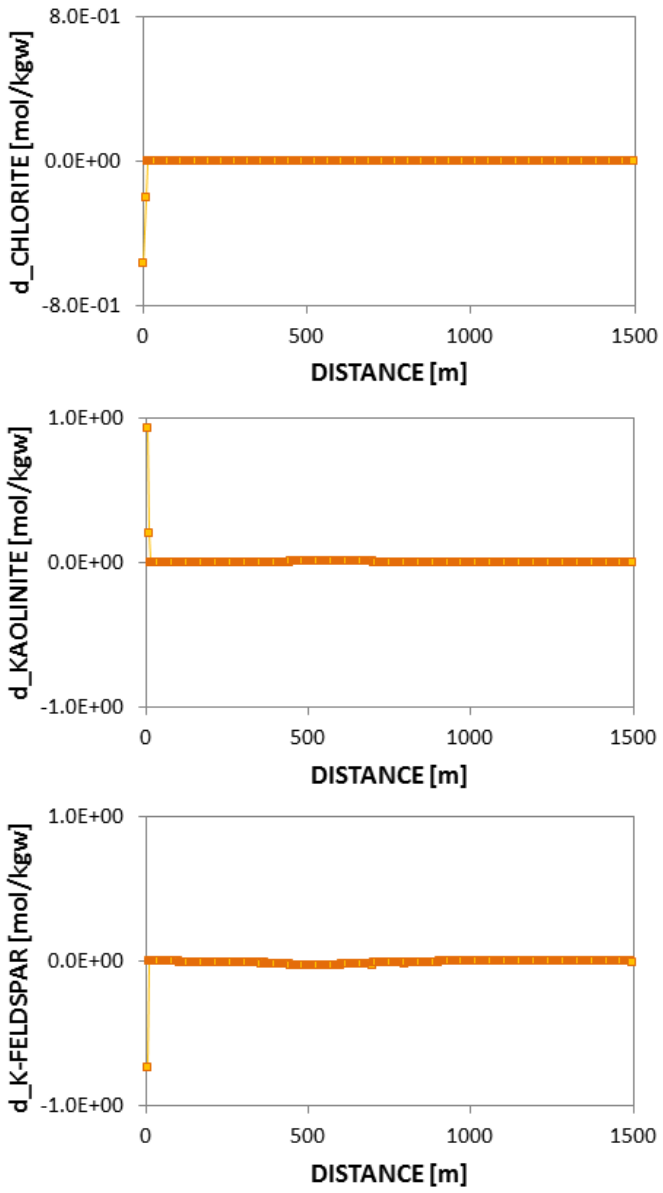

Figure 5.12: *Amounts of chlorite, kaolinite and K-feldspar calculated for Thisted geothermal reservoir after 20 years of plant operation. Mineral precipitation and dissolution are indicated by positive and negative values, respectively.*

The amount of K-feldspar, kaolinite and chlorite precipitated or dissolved upon injection of cooled formation water at the three geothermal plants are shown in Figures 5.10, 5.11 and 5.12. The major process observed at all studied geothermal plants is K-feldspar dissolution. The dissolution progresses further into the reservoirs with time. K-feldspar alters to kaolinite and/or chlorite. The described processes occur mainly at the parts of the reservoirs that is cooled down due to the injection of cold brines at Sønderborg and Margretheholm site. However, the influence of these transformation processes on the performance of the geothermal plants can be neglected, as they probably do not influence significantly reservoirs porosity. Another mineral dissolved at low temperatures at Sønderborg and Margaretholm is illite, although in small quantities, as it constitutes <1% of reservoir composition. Quartz and the

remaining Al-bearing minerals (albite, K-mica) are neither precipitated nor dissolved in the studied reservoirs. Dissolution of small amounts of albite (0.4 mol/kgw) occurred only during the first year of operation at Margretheholm, in the proximity of an injection well.

5.4 Barite precipitation in the injection wells

Modelling of the injection of cooled formation water into the reservoir at Margretheholm, Sønderborg and Thisted geothermal plants indicate that barite may precipitate in the reservoir near the injection well, particularly at Margretheholm. Therefore, barite precipitation is investigated in more details, and the possibility of barite precipitation in the injection wells is investigated.

Even if the formation of barite is thermodynamically possible, barite precipitation is kinetically controlled. The precipitation rate depends on several parameters such as the temperature, the saturation index, ionic strength and the presence (or absence) of surface area on which the mineral grows. It was first attempted to simulate the barite precipitation with MARTHE-PHREEQC by using the nucleation model developed by Dideriksen et al. (in prep). Unfortunately, the model cannot be used in the parallel environment in MARTHE-PHREEQC (i.e. issues with GET and PUT options of PHREEQC, see Parkhurst and Appelo, 2013 for more details) and was forsaken in the present MARTHE-PHREEQC study. Thus, the possibility of barite nucleation in the injection wells was checked in 1D transport calculations using PHREEQC 3.0 and the pitzer database.

Results show that barite nucleation appears to be unlikely in the injection wells at Sønderborg and Thisted geothermal plants but is possible in the injection well at Margretheholm geothermal plant (Figure 5.13). Implementation of nucleation in the modelling indicate that the nucleation is unexpected for saturation indices below ~1. Saturation indices (i.e. log Q/K) are 0.5 (15 °C), 0.8 (15 °C) and 1.2 (20 °C) after heat extraction for the Sønderborg, Thisted and Margretheholm geothermal plants, respectively. Therefore, barite nucleation appears to be unlikely in the Sønderborg and Thisted geothermal plants and occurs in the Margretheholm geothermal plant (Figure 5.13). Barite quantities nucleated at Margaretholm are small. Simulated weekly maximal growth of barite crystals equals 8.64E-3 nm (Figure 5.13.), which gives an annual growth of 0.45 nm. The results also indicate that nucleation of barite at Margretheholm is a fast process that may very well occur immediately after cooling of the formation water in the heat exchanger.

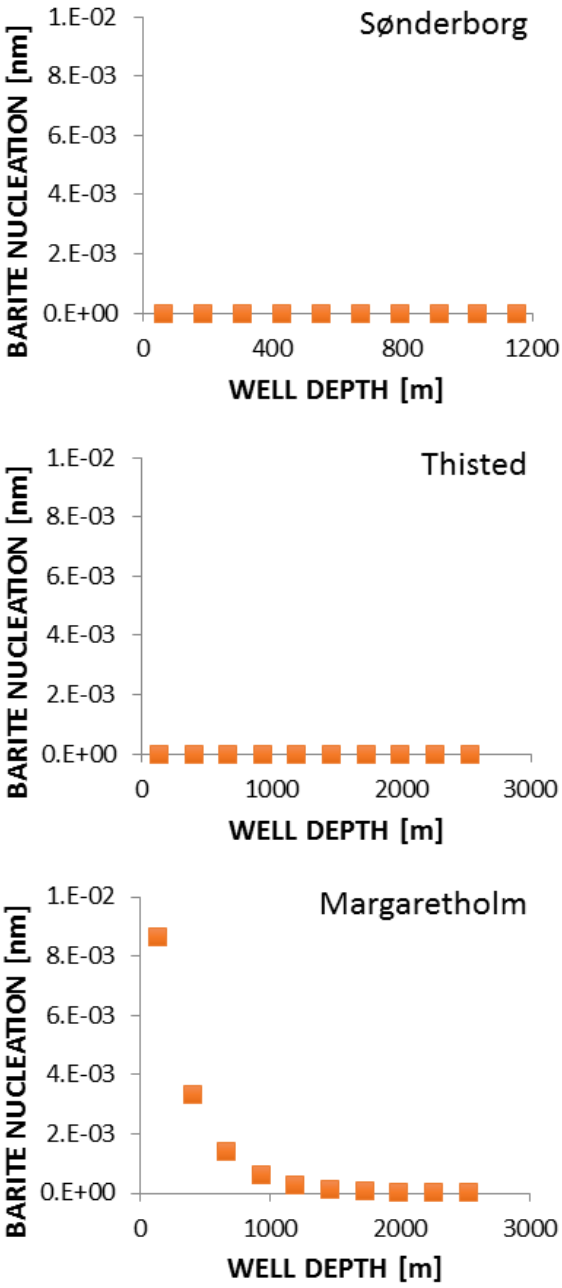

Figure 5.13: *Results of the barite nucleation modelling at the injection wells. The y-axis indicate the thickness in nm of the expected layer of barite precipitated.*

5.5 Modelled results versus experienced problems

The geochemical modelling performed in this study suggests that celestine and particularly barite precipitation may represent the potentially highest risk at Margretheholm geothermal plant. Particularly precipitation of barite is a fast process and the modelling results show that barite may precipitate fast in the injection well or in the reservoir. Thus, the modelling results indicate that barite may potentially precipitate anywhere in the geothermal loop after the heat exchanger. It should, however, be noted that the nucleation model applied in this study is

calibrated at a temperature and pressure range between 75°C - 85°C and 110 – 160 bar and therefore the calculations are associated with a certain uncertainty.

Only small amounts of alternating barite–celestite have been detected in particles collected from the plant at Margretheholm and precipitation of barite at Margretheholm has previously been ruled out as a significant process partly due to a slow barite precipitation kinetics (Laier, 2002). However, Bhandri et al. 2016 found that at a given temperature barite nucleation rates increases with increasing pressure indicating that barite nucleation is most favourable at the bottom of the injection well. Thus if the precipitation of barite occurs at the bottom of the injection well or in the reservoir, the barite particles are not detected in the above ground investigations. Thus, this study shows that precipitation of barite at Margretheholm cannot be excluded as part of the reasons for the observed injectivity problems at the Margretheholm geothermal plant.

It has been suggested that the injection problems at Margretheholm are mainly caused by precipitation of metallic Pb due to galvanic corrosion (Laier, 2015b, 2015c, 2015d). A small increase in the concentration of aqueous Pb just before the injection well compared with the Pb content in the formation water at the well head at the production well may reflect corrosion occurring in the plant (Figure 3.1). The galvanic corrosion depends on steel composition, salinity of fluid, pH, turbulent flow etc. (e.g. Bozau et al. 2015, Ng et al. 2018). Application of corrosion inhibitors was tested at Margretheholm, though the effect was not thoroughly verified (Troels Laier, pers. comm. 2019).

Geochemical modelling of the water at the Sønderborg plant suggests insignificant mineral precipitations. Thus the amount of e.g. barite precipitation in the reservoir upon injection of cooled formation water at Sønderborg geothermal plant is expected to be smaller than that at Thisted geothermal plant, that has not experienced injectivity problems. The modelling results thus suggest that other causes than scaling may also be responsible for the injectivity problems at Sønderborg. Several causes for the injection problems at Sønderborg have been proposed including a non-optimal installation of the gravel packs (van der Post 2019), high corrosion rates in the injection well (Mathiesen 2019) combined with mill scales on the inside of all tubing (Mathiesen et al. 2019), sulphate reduction resulting in zink- and lead-sulphide precipitates and possibly biofilm formation (Laier 2016). Such operational problems cannot be predicted or addressed from the geochemical modelling.

The Schoeller diagram (Figure 3.2) indicates an increase in the concentration of iron at the injection well compared to the content at the well head in the production well indicating that corrosion may occur in the geothermal plant. High corrosion rates have been observed in the injection well (Mathiesen 2019) which may be associated with oxygen ingress at the injection well pump. Oxygen-promoted corrosion in this part of the plant facility could promote an increase in the Fe content in the geothermal water and potential precipitation of iron-oxides/hydroxides that may clog the pore throats in the reservoir. The Schoeller diagram (Figure 3.2) also reveals a significant decrease in the concentration of aqueous Zn between the production well and injection well at Sønderborg geothermal plant. Suspended zink- and lead sulphides have been identified in the water at Sønderborg geothermal plant (Laier, 2015) and thus precipitation of these sulphides is likely. This process is promoted by a high sulphate

content in the formation water and a microbiologically facilitated reduction of sulphate to sulphide as confirmed by the identification of DNA from sulphate-reducing bacteria in the bag filters.

6. Conclusions

Geochemical modelling of the production and injection water from the Sønderborg and Thisted geothermal plants suggests insignificant mineral precipitations in the injection wells and upon injection of the cooled formation water into the reservoir at these plants. In contrary, the production and injection water compositions from the Margretheholm plant suggest that barite and celestine precipitation may occur after the heat extraction. Precipitation of celestine is modelled to occur c. 50-100 m from the injection well. Precipitation of barite on the other hand occur instantaneously whether the process is modelled in the injection well or in the reservoir. It is thus unclear whether barite precipitates immediately after cooling of the formation water in the heat exchanger. If the barite precipitates are not captured in the filters before injection into the reservoir, precipitation in the reservoir may affect the injection of cooled water by clogging the porosity of the reservoir rock.

The geochemical modelling performed in this project considers the risk of scaling due to the heat extraction, and several processes such as the formation of biofilm, corrosion processes and transport of particles have not been taken into account because of a lack of data reported in the model databases and current software capabilities (e.g. transport of eroded particles). The results indicate that scaling may only to a limited extend account for the injectivity problems observed at Margretheholm and Sønderborg geothermal plants and that there may be other reasons for the injectivity problems e.g. defect gravel pack, galvanic corrosion etc. or more likely a combination of several causes.

7. Recommendations for further studies

Although much information is achieved from the geochemical modelling in this project, it is a first attempt to model the geochemical reactions occurring in the Danish geothermal plants and as such afflicted with uncertainties and many assumptions. Recommendations for further studies therefore include:

1. Further geochemical modelling
   Further and more detailed geochemical modelling could improve our understanding of the chemical reactions occurring in the reservoir at the Danish geothermal plants. In this study equilibrium has been assumed with respect to a large number of minerals e.g. carbonates, and further geochemical modelling should therefore include the kinetics of these minerals. Furthermore, the precipitation of barite in the geothermal plant should be modelled in more details.

2. Potential for barite precipitation in the reservoir.
   The risk of barite precipitation in the reservoir could be tested by laboratory experiments at reservoir pressure where core material is flooded with brine super saturated with respect to barite. Barite precipitation is identified by measuring any decrease in the barium and sulphate concentration and by petrographic analysis. If measurements allow any changes in the permeability could be monitored during the experiment. The laboratory experiment would be complimented by geochemical modelling e.g modelling of the barite nucleation rate.

3. Stable isotopic composition
   An indirect measurement of the stable isotopic composition of the formation water can be obtained from oxygen and carbon isotopic measurements of authigenic phases at several different burial depths. At present, we have focused only on obtaining the temperature estimates at maximum burial depth. However, if cementing phases forming at shallower burial depth are measured, the development from depositional water towards formation water can be understood. This would improve the predictability of formation water composition in undrilled areas.

4. Radiogenic isotopic composition
   Measurements of radiogenic composition of new formation water samples would allow age dating of the formation water. This would improve the understanding mixing of formation waters of different origin. Unfortunately, no previous measurements have been obtained, however it ought be initiated when the possibility comes.

8. References

Andritsos, N., Karabelas, A.J., Koutsoukos, P. 2002. Scale formation in geothermal plants. International Summer School on Direct Application of Geothermal Energy, 179-189.

Andritsos, N., Karabellas, A.J. 1991. Sulfide scale formations and control: The case of lead sulphide. Geothermics 20, 343-353.

Bhandari N, Kan, A.T., Zhan F., Dai, Z. Yan, F., Ruan G., Zhang, Z., Liu, Y., van Eldik, R., Tomson, M. B. 2016. Mineral precipitation kinetics: Assessing the effect of hydrostatic pressure and its implication on the nucleation mechanism. Crystal Growth & Design 16, 4846 – 4854.

Blanc, P., Lassin, A., Piantone, P., Azaroual, M., Jacquemet, N., Fabbri, A., Gaucher, E.C., 2012. Thermoddem: A geochemical database focused on low temperature water/rock interactions and waste materials. Applied Geochemistry 27, 2107-2116.

Bozau, E., Häußler, S., van Berk, W., 2015. Hydrogeochemical modelling of corrosion effects and barite scaling in deep geothermal wells of the North German Basin using PHREEQC and PHAST. Geothermics 53, 540-547

Clemmensen, L.B. 1985: Desert sand plain and sabkha deposits from the Bunter Sandstone Formation (L. Triassic) at the northern margin of the German Basin. Geologische Rundschau 74, 519–536.

Dansk Fjernvarme. 2019. https://www.geotermi.dk/geotermiske-anlaeg/

Debure, M., Andreazza, P., Canizarès, A., Grangeon, S., Lerouge, C., Mack, P., Madé, B., Simon, P., Veron, E., Warmont, F., Vayer, M., 2017. Study of Iron-Bearing Dolomite Dissolution at Various Temperatures: Evidence for the Formation of Secondary Nanocrystalline Iron-Rich Phases on the Dolomite Surface. ACS Earth and Space Chemistry 1, 442-454.

Demir, M.M., Baba, A., Atilla, V., Inanli, M. 2014. Types of the scaling in hyper saline geothermal system in northwest Turkey. Geothermics 50, 1 – 9.

Dideriksen, K., Zhen-Wu, B.Y., Dobberschütz, S., Rodríguez-Blanco, J.D., Raahauge, P.J., Ataman, E., Oelkers, E.H., Stipp, S.L.S., in prep. A model for nucleation and growth for use in 1 PHREEQC: Prediction of barite formation in an oil well.

Energy Supply. 2016. Geotermisk boring I Sønderborg driller. https://www.energy-supply.dk/article/view/237448/geotermisk_boring_i_sonderborg_driller

Energistyrelsen 2019. https://ens.dk/ansvarsomraader/geotermi/geotermianlaeg-i-drift

Erlström, M. 2017. The Lund Geothermal System. Background, design and review of operational experiences. Geotherm Project, Status Report WP 3.2c and WP5.1, 31p. (Internal Report prepared by Lund University for GEUS.).

Gysi, A.P., Stefánsson, A., 2012. CO2-water–basalt interaction. Low temperature experiments and implications for CO2 sequestration into basalts. Geochimica et Cosmochimica Acta 81, 129-152.

Holmslykke, H.D., Schovsbo, N.H., Kristensen, L., Weibel, R., Nielsen, L.H., 2019. Characterising brines in deep Mesozoic sandstone reservoirs, Denmark. Geological survey of Denmark and Greenland Bulletin 43.

Kristensen, L., Hjuler, M. L., Frykman, P., Olivarius, M., Weibel, R., Nielsen, L. H., Mathiesen, A. 2016. Pre-drilling assessments of average porosity and permeability in geothermal reservoirs of the Danish area. Geothermal Energy 4:6, 27p.

Lach, A., André, L., Guignot, S., Christov, C., Henocq, P., Lassin, A., 2018. A Pitzer Parametrization To Predict Solution Properties and Salt Solubility in the H–Na–K–Ca–Mg–NO 3 –H 2 O System at 298.15 K. Journal of Chemical and Engineering Data 63, 787 - 800.

Laier, T., Weibel, R. 2011. Recovery of reservoir permeability by acid injection in the Margretheholm-1 geothermal well – potential risk assessment. Geolgical Survey of Denmark and Greenland Bulletin 2011/102, 31p.

Laier, T.2014. Årsag til injektionsproblemer I MAH-1, vurderet ud partikelundersøgelser. GEUS-NOTAT, 22p.

Laier, T. 2015. Membranfilterprøver, viser zinksulfid og blysulfid i Sønderborg geotermiske anlæg. GEUS Notat, 20. april 2015, 17p.

Laier, T. 2015a. SEM-EDS undersøgelse af membranfilterprøver far MAH-2 geotermiske boring. GEUS letter, 11p.

Laier, T. 2015b. Blypartikler i posefiltre på GDA skyldes muligvis midlertidige blyudfældninger i anlæg. GEUS letter, 10p

Laier, T. 2015c Bly i belægninger og posefiltre på GDA. GEUS letter, 8p.

Laier, T. 2015d Lead in formation water causes problems in geothermal exploitation at Margretheholm, GEUS letter, 21p.

Laier, T. 2016. Mikrobiel sulfiddannelse i Sønderborgs geotermiske anlæg. GEUS Notat, 25. februar 2016, 10p.

Laier, T. 2002. Vurdering af udfældningsrisici ved geotermisk production fra Margretheholm. MAH-1A. Beregning af mætningsindeks for mineraler i saltvand fra Danmarks dybere underground. GEUS rapport 2002/95.

Lasaga, A.C., 1981. Transition state theory. Rev. Mineral.;(United States) 8.

Lassin, A., André, L., Lach, A., Thadée, A.-L., Cézac, P., Serin, J.-P., 2018. Solution properties and salt-solution equilibria in the H-Li-Na-K-Ca-Mg-Cl-H2O system at 25 °C: A new thermodynamic model based on Pitzer's equations. Calphad 61, 126-139.

Mathiesen, T. 2019. Results of on-site monitoring campaign and parametric laboratory testing. GEOTHERM Milestone Report M5.4, 41p.

Ng, D.Q., Chen, C.Y., Lin, Y.P. 2018. A new scenario of lead contamination in potable water distribution systems: Galvanic corrosion between lead and stainless steel. Science of the Total Environment 637, 1423–1431.

Nitschke, F., Scheiber, J., Kramar, U., Neumann, T. 2014. Formation of alternating layered Ba-Sr-sulfate and Pb-sulfide scaling in hte geothermal plant of Soultz-sous-Forêts. Neues Jahrbuch für Mineralogie, Abhandlungen 191/2, 145–156.

Olivarius, M., Laier, T., Knudsen, C., Malkki, S.H., Thomsen, T.B., Serre, S.H., Kristensen, L., Willumsen, M.E., Nielsen, L.H. 2018. Source and occurrence of radionuclides in geothermal water. With focus on the Margretheholm geothermal plant. Geological Survey of Denmark and Greenland Bulletin 2018/41, 77p.

Oliveira, D.F., Santos, R.S., Machado, A.S., Silva, A.S.S., Anjos, M.J., Lopes, R.T., 2019. Characterization of scale deposition in oil pipelines through X-Ray Microfluorescence and X-Ray microtomography. Applied Radiation and Isotopes 151, 247-255.

Olsen, H., 1987. Ancient ephemeral stream deposits: a local terminal fan model from the Bunter Sandstone Formation (L. Triassic) in the Tønder-3, -4 and -5 wells, Denmark. In: Frostick, L., Reid, I. (Eds.), Desert Sediments: Ancient and Modern. Geological Society Special Publication 35, 69– 86.

Palandri, J., Kharaka, Y., 2004. A Compilation of Rate Parameters of Water-Mineral Interaction Kinetics for Application to Geochemical Modeling. 1068, 71

Parkhurst, D.L., Appelo, C., 2013. Description of input and examples for PHREEQC version 3—a computer program for speciation, batch-reaction, one-dimensional transport, and inverse geochemical calculations. US geological survey techniques and methods, book 6, 497.

Pastrik, N., Förster, A. 2017. GEOTHERM – Geothermal energy from sedimentary reservoirs – Removing obstacles for large scale utilization. Report (milestone M3.1 and M5.1). Experiences gained from German geothermal plants: a synopsis, 60p. (Internal report prepared by GFZ for GEUS).

Rimstidt, J.D., Barnes, H.L., 1980. The kinetics of silica-water reactions. Geochimica et Cosmochimica Acta 44, 1683-1699.

Rodríguez-Morillas, N., Playa, E., Travé, A., Martín-Martín, J., 2013. Diagenetic processes in a partially dolomitized carbonate reservoir: Casablanca oil field, Mediterranean Sea, offshore Spain. Geologica Acta 11, 195-214.

Thiéry, D., 2015. Modélisation 3D du Transport Réactif avec le code de calcul MARTHE v7.5 couplé aux modules géochimiques de PHREEQC, in: BRGM/RP-65010-FR, R. (Ed.), Orléans, France, pp. 164, available at http://infoterre.brgm.fr/rapports/RP-65010-FR.pdf .

Trémosa, J., Marty, N., Bouchot, V. 2017. Experience with geothermal plants in France, 33p. (Internal Report prepared by BRGM for GEUS).

Trémosa, J., Castillo, C., Vong, C.Q., Kervévan, C., Lassin, A., Audigane, P., 2014. Long-term assessment of geochemical reactivity of CO2 storage in highly saline aquifers: Application to Ketzin, In Salah and Snøhvit storage sites. International Journal of Greenhouse Gas Control 20, 2-26.

Vinsome, P., Westerveld, J., 1980. A simple method for predicting cap and base rock heat losses in thermal reservoir simulators. Journal of Canadian Petroleum Technology 19.

Vosgerau, H., Mathiesen, A., Kristensen, L., Andersen, M.S., Hjuler, M.L., Laier, T. 2015C. Det geotermiske screeningsprojekt. Hillerød-lokaliteten. Danmark og Grønlands Geologiske Undersøgelse Rapport 2015/15, 33p.

Vosgerau, H., Mathiesen, A., Kristensen, L., Andersen, M.S., Hjuler, M.L., Laier, T. 2015B. Det geotermiske screeningsprojekt. Sønderborg-lokaliteten. Danmark og Granlands Geolgoiske Undersøgelse Rapport 2015/33, 30p.

Vosgerau, H., Mathiesen, A., Kristensen, L., Andersen, M.S., Hjuler, M.L., Laier, T. 2015A. Det geotermiske screeningsprojekt. Sønderborg-lokaliteten. Danmark og Grønlands Geologiske Undersøgelse Rapport 2015/47, 31p.

Wanner, C., Eichinger, F., Jahrfeld, T., Diamond, L.W. 2017. Causes of abundant calcite scaling in geothermal wells in Bavarian Molasse Basin, Southern Germany. Geothermics 70, 324 – 338.

Weibel, R., Friis, H. 2004. Opaque minerals as keys for distinguishing oxidising and reducing diagenetic conditions in the Lower Triassic Bunter Sandstone, North German Basin. Sedimentary Geology 169, 129–149.

Weibel, R., Olivarius, M., Kristensen; L., Friis, H., Hjuler, M. L., Kjøller, C., Mathiesen, A., Nielsen, L. H. 2017. Predicting permeability of low enthalpy geothermal reservoirs: A case study from the Upper Triassic−Lower Jurassic Gassum Formation, Norwegian–Danish Basin. Geothermics 65, 135-157.

Zhen-Wu, B.Y., Dideriksen, K., Olsson, J., Raahauge, P.J., Stipp, S.L.S., Oelkers, E.H., 2016. Experimental determination of barite dissolution and precipitation rates as a function of temperature and aqueous fluid composition. Geochimica et Cosmochimica Acta 194, 193-210.